

ORNL/TM-2015/142

# Kinetics of Chronic Oxidation of NBG-17 Nuclear Graphite by Water Vapor



Cristian Contescu  
Timothy Burchell  
Robert Mee

**April 2015**

## DOCUMENT AVAILABILITY

Reports produced after January 1, 1996, are generally available free via US Department of Energy (DOE) SciTech Connect.

**Website** <http://www.osti.gov/scitech/>

Reports produced before January 1, 1996, may be purchased by members of the public from the following source:

National Technical Information Service  
5285 Port Royal Road  
Springfield, VA 22161  
**Telephone** 703-605-6000 (1-800-553-6847)  
**TDD** 703-487-4639  
**Fax** 703-605-6900  
**E-mail** info@ntis.gov  
**Website** <http://www.ntis.gov/help/ordermethods.aspx>

Reports are available to DOE employees, DOE contractors, Energy Technology Data Exchange representatives, and International Nuclear Information System representatives from the following source:

Office of Scientific and Technical Information  
PO Box 62  
Oak Ridge, TN 37831  
**Telephone** 865-576-8401  
**Fax** 865-576-5728  
**E-mail** reports@osti.gov  
**Website** <http://www.osti.gov/contact.html>

This report was prepared as an account of work sponsored by an agency of the United States Government. Neither the United States Government nor any agency thereof, nor any of their employees, makes any warranty, express or implied, or assumes any legal liability or responsibility for the accuracy, completeness, or usefulness of any information, apparatus, product, or process disclosed, or represents that its use would not infringe privately owned rights. Reference herein to any specific commercial product, process, or service by trade name, trademark, manufacturer, or otherwise, does not necessarily constitute or imply its endorsement, recommendation, or favoring by the United States Government or any agency thereof. The views and opinions of authors expressed herein do not necessarily state or reflect those of the United States Government or any agency thereof.

Advanced Reactor Technology Program

**KINETICS OF CHRONIC OXIDATION OF NBG-17  
NUCLEAR GRAPHITE BY WATER VAPOR**

**Cristian Contescu  
Timothy Burchell**

Oak Ridge National Laboratory

**Robert Mee**

University of Tennessee, Knoxville

April 2015

Prepared by  
OAK RIDGE NATIONAL LABORATORY  
Oak Ridge, Tennessee 37831-6283  
managed by  
UT-BATTELLE, LLC  
for the  
US DEPARTMENT OF ENERGY  
under contract DE-AC05-00OR22725



## **ACKNOWLEDGMENT**

This work is funded by the U.S. Department of Energy, Office of Nuclear Energy Science and Technology, under contract DE-AC05-00OR22725 with Oak Ridge National Laboratory managed by UT-Battelle, LLC.



## CONTENTS

	<b>Page</b>
<b>LIST OF FIGURES</b> .....	ix
<b>LIST OF TABLES</b> .....	xi
<b>LIST OF ABBREVIATIONS</b> .....	xiii
<b>EXECUTIVE SUMMARY</b> .....	xv
<b>1. INTRODUCTION</b> .....	1
<b>2. EXPERIMENTAL SETUP AND EQUIPMENT PERFORMANCE</b> .....	3
<b>3. MATERIALS</b> .....	5
3.1 GRAPHITE SAMPLES .....	5
3.2 GASES.....	8
<b>4. PROCEDURE</b> .....	9
4.1 TEST CONDITIONS .....	9
4.2 PREPARATION OF SPECIMENS BEFORE TESTS .....	9
4.3 OXIDATION TEST PROCEDURE.....	9
4.4 SPECIMEN CHARACTERIZATION AND DATA SAVING AFTER TESTS .....	10
4.5 DATA REDUCTION .....	11
<b>5. DATA ANALYSIS</b> .....	13
5.1 LANGMUIR-HINSHELWOOD KINETIC MODEL.....	13
5.2 DETERMINATION OF KINETIC PARAMETERS.....	14
<b>6. DISCUSSION OF RESULTS</b> .....	19
<b>7. CONCLUSION AND FUTURE WORK</b> .....	21
<b>REFERENCES</b> .....	23
<b>ANNEX</b> .....	25
<b>Table A-1</b> Physical properties of NBG-17 specimens before and after oxidation .....	27
<b>Table A-2</b> Experimental oxidation rates and corresponding conditions .....	29
<b>Table A-3</b> Fitted parameter estimates and standard errors provided by SAS .....	35



## LIST OF FIGURES

Figure	Page
1. Schematic of experimental setup for oxidation experiments with low concentrations of water in high purity helium.....	3
2. Cutting diagram of NBG-17 billet .....	5
3. Cutting diagram of the ORNL sub-section of NBG-17 billet.....	6
4. Specimen extraction scheme for NBG-17 oxidation by water.....	7
5. Example of processed TG data recorded in a 24 hour long run where water pressure was kept constant (30 Pa) and the temperature was increased from 800 to 1100 °C.....	11
6. Example of processed TG data recorded in a 72 hour long run where temperature was kept constant (850 °C) and water vapor pressure and hydrogen pressure were varied.....	12
7. Oxidation rates predicted with parameters in Table 1 versus observed rates at $P_{H_2}=0$ .....	16
8. Oxidation rates predicted with parameters in Table 1 versus observed rates at $P_{H_2}=26$ Pa.....	16
9. Comparison between oxidation rates predicted with parameters in Table 1 and actual measured rates .....	17



## LIST OF TABLES

<b>Table</b>	<b>Page</b>
1. L-H fitted parameters using all valid 286 observations .....	15
2. Summary of L-H parameters for three nuclear graphites.....	19

## ANNEX

<b>Table A-1</b>	Physical properties of NBG-17 specimens before and after oxidation .....	27
<b>Table A-2</b>	Experimental oxidation rates and corresponding conditions .....	29
<b>Table A-3</b>	Fitted parameter estimates and standard errors provided by SAS .....	35



## LIST OF ABBREVIATIONS

AG	against grain
CALISTO	software (of TAG instrument)
DOE	Department of Energy
DTG	derivative of thermogravimetric function (TG curve)
H-451	nuclear graphite grade used in the Fort Vrain reactor (U.S.)
HTGR	high temperature gas-cooled reactor
HTR	high temperature reactor
IG-110	grade of nuclear graphite manufactured by Toyo Tanso in Japan
INL	Idaho National Laboratory
L-H	Langmuir-Hinshelwood (kinetic mechanism, equation)
NGNP	Next Generation Nuclear Plant
MF	mass flow (controller)
ML	maximum likelihood
MLE	maximum-likelihood estimate
NBG-17	grade of nuclear graphite manufactured by SGL Carbon Group in Germany
NBG-18	grade of nuclear graphite manufactured by SGL Carbon Group in Germany
ORNL	Oak Ridge National Laboratory
QUADERA	software (of the mass spectrometer)
PBMR	Pebble Bed Modular Reactor
PCEA	grade of nuclear graphite manufactured by GrafTech International in the U.S.
ppm	parts per million (concentration units)
ppmv	parts per million (in volume units)
ppt	parts per trillion (concentration units)
R&D	research and development
Ref., ref.	reference
TAG	thermo-analyseur gravimetrique (thermogravimetric analyzer)
TG	thermogravimetric function (temperature vs weight)
UHP	ultra-high purity
VHTR	very high temperature reactor
WG	with grain



## EXECUTIVE SUMMARY

This report presents the results of kinetic measurements during accelerated oxidation tests of NBG-17 nuclear graphite by low concentrations of water vapor and hydrogen in ultra-high purity helium. The objective is to determine the parameters in the Langmuir-Hinshelwood (L-H) equation describing the oxidation kinetics of nuclear graphite in the helium coolant of high temperature gas-cooled reactors (HTGR). Although the helium coolant chemistry is strictly controlled during normal operating conditions, trace amounts of moisture (predictably  $< 0.2$  ppm) cannot be avoided. Prolonged exposure of graphite components to water vapor at high temperature will cause very slow (chronic) oxidation over the lifetime of graphite components. This behavior must be understood and predicted for the design and safe operation of gas-cooled nuclear reactors. The results reported here show that, in general, oxidation by water of graphite NBG-17 obeys the L-H mechanism, previously documented for other graphite grades. However, the characteristic kinetic parameters that best describe oxidation rates measured for graphite NBG-17 are different from those reported previously for grades H-451 (General Atomics, 1978) and PCEA (ORNL, 2013). In some specific conditions, certain deviations from the generally accepted L-H model were observed for graphite NBG-17. This graphite is manufactured in Germany by SGL Carbon Group and is a possible candidate for the fuel elements and reflector blocks of HTGR.



## 1. INTRODUCTION

Nuclear grade graphite is the moderator and a major structural component of High Temperature Gas-Cooled Reactors (HTGR). Graphite is chemically stable at high temperatures in inert helium (He) and reducing environments, but it becomes gasified by oxidizing impurities (oxygen, carbon dioxide, water) that might be present in the HTGR helium coolant. Water is the main oxidizing impurity in He coolant, albeit in very low concentrations. The water partial pressure varies between different HTGR designs but is expected not to exceed 1–1.5 Pa at total helium pressures of 7–9 MPa [1,2,3,4,5,6]. The oxidation reaction of carbon by water produces carbon monoxide and hydrogen:



This reaction is not energetically favorable at temperatures below  $\sim 700$  °C but may play an important role in graphite gasification at higher temperatures, particularly at high water vapor pressures [7].

Under normal operating conditions, oxidation is predictably very slow (chronic) and limited to the surface of graphite components. Predictions show that chronic degradation of graphite properties caused by oxidation by moisture in the coolant circuit will not significantly affect the integrity of graphite components during normal operating conditions. However, these predictions are based on accelerated oxidation measurements made on graphite grade H-451 in 1978 at General Atomics Company [8]. This grade of nuclear graphite is no longer available, and little is known about the oxidation properties of the new grades regarded as candidates for gas-cooled reactors in the United States.

Recent results obtained at Oak Ridge National Laboratory (ORNL) showed that the microstructural characteristics of various graphite grades have significant effects on their chemical reactivity. This has been documented for oxidation by air in conditions that simulate the improbable event of an air-ingress accident [9]. Moreover, an accelerated kinetic study of oxidation by moisture of PCEA graphite produced in the U.S. by GrafTech International showed differences from the results known for the historic grade H-451 [10]. Although the general kinetic mechanism, known as the Langmuir-Hinshelwood (L-H) mechanism [11,12,13,14], operates for both graphite types, the parameters describing the effects of temperature and gas composition on the reaction rates are different. Extrapolation of accelerated oxidation results to the normal operating conditions in HTGR indicates that PCEA graphite would oxidize slightly faster than H-451 graphite at low temperatures (750–800 °C) and slightly slower at higher temperatures (900–950 °C). Consequently, it can be predicted that at low temperatures, PCEA would develop a narrower oxidation layer on exposed surfaces than what was predicted for graphite H-451. However, the same predictions show that the oxidation layer would penetrate deeper under the surface of PCEA graphite compared to graphite H-451 [15,16,17]. These crude predictions need further confirmation based on results of effective diffusivity measurements of water vapor from He. Recent experimental results on water vapor transport properties of two graphite grades, PCEA and NBG-17, were reported in a parallel study completed at ORNL [18].

This report presents results of accelerated oxidation tests by water vapor of nuclear graphite grade NBG-17. Considered as a candidate for HTGR, this vibrationally molded graphite is manufactured by SGL Carbon (Germany/France). The fuel blocks in prismatic reactors have cooling channels separated by rather small graphite walls; therefore, the optimal graphite material should have small grain size. According to the manufacturer, the *maximum* grain size in graphite NBG-17 is 0.8 mm. This is similar to the maximum grain size of PCEA (0.8 mm), half the maximum grain size of NBG-18 (1.6 mm), and much larger than that of IG-110 (0.04 mm) [19, 20]. The *average* grain size reported for NBG-17 is 0.3 mm [21]. According to mercury porosity measurements, the pore size distribution in NBG-17 is bimodal,

with the narrowest pores of about 0.01  $\mu\text{m}$  and the largest size pores distributed between 5 and 30  $\mu\text{m}$ . The cumulative pore volume is about 14 % of the graphite bulk volume [22]. This study followed the same method and experimental setup as previously used for accelerated oxidation studies of graphite PCEA [23]. The experiments were designed to be feasible in laboratory conditions while bearing relevance to normal operation of HTGR, and to provide high quality results with reasonable time and budget resources.

## 2. EXPERIMENTAL SETUP AND EQUIPMENT PERFORMANCE

The experimental setup diagram is shown in Figure 1. The main components are the gas delivery system of the oxidant gas with controlled composition and flow rate, the thermogravimetric analyzer (TAG 16/18 from SETARAM, France), and the mass spectrometer (DSC 350 from Pfeiffer, USA). A detailed description of these components was provided in a previous report [23].

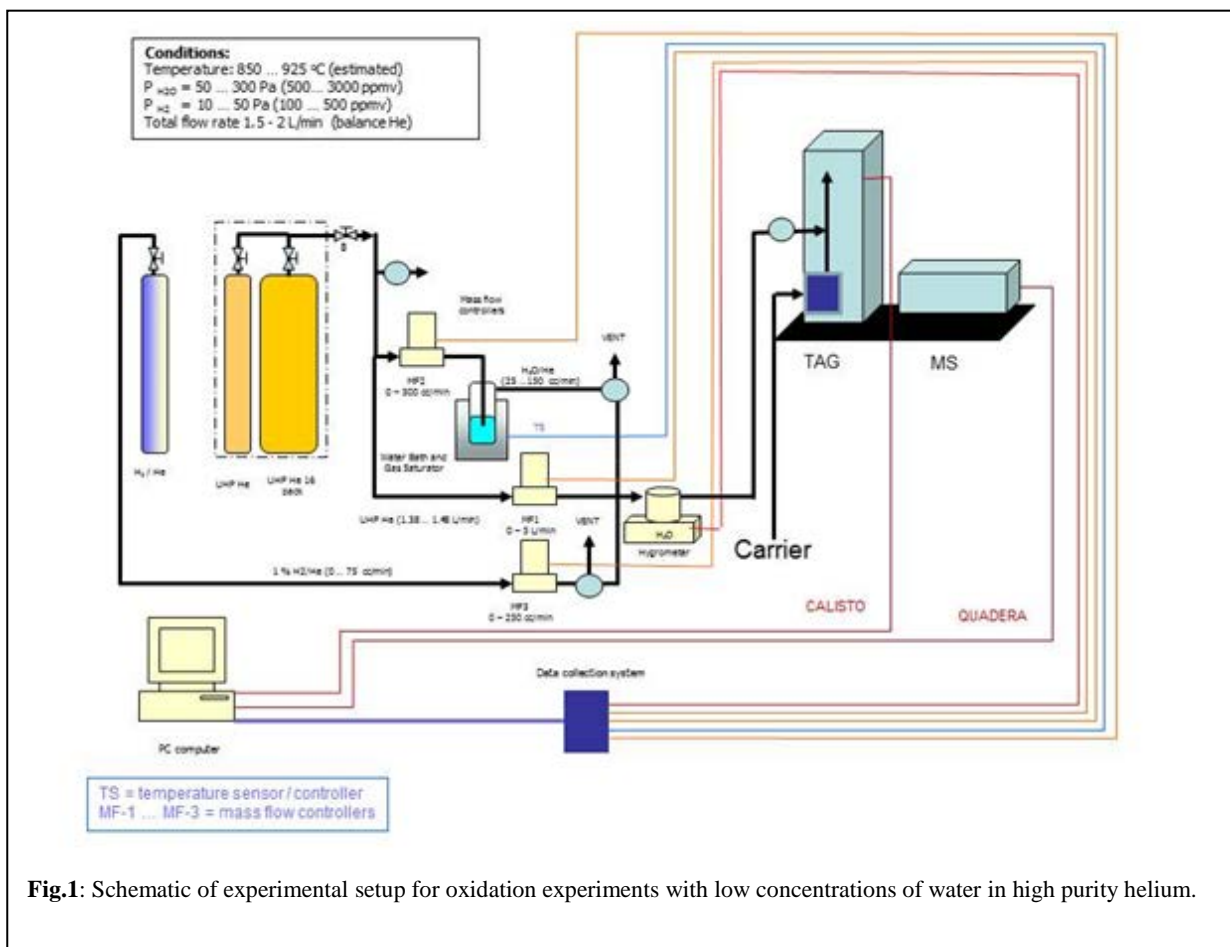


**Fig.1:** Schematic of experimental setup for oxidation experiments with low concentrations of water in high purity helium.

The ultra-high purity (UHP) helium used in this study (Air Liquide, USA) contains < 0.1 ppm water and < 0.5 ppm oxygen, with balance He (>99.999 %), based on the analysis certificate provided by Air Liquide. Water vapor was introduced by bubbling a split He line through plasma-grade water (Fisher Scientific) maintained at constant ( $\pm 0.05$  °C) temperature. The source of hydrogen added in some experiments was a certified  $H_2/He$  mixture with 1 % by volume  $H_2$  (certified by Air Liquide, USA). The water content in the mixed gas obtained by mixing dry He, wet He, and  $H_2/He$  lines was measured by a chilled mirror hygrometer (CR-4 from Buck Research Instruments, LLC, Boulder, CO) placed before the

thermogravimetric analyzer. The flow rates in the three gas lines (dry He, moist He, and H<sub>2</sub>/He mixture) were regulated by mass flow controllers (Sierra Instruments) and monitored by a LabView application. The same application also collected hygrometer data (dew point temperature and internal pressure), barometric conditions in the lab (temperature, humidity, and atmospheric pressure) measured by a wall-mounted instrument (Control Company, USA), and the temperature of the water bath (Fisher Scientific, USA) holding the He bubbler. When corrected for the barometric pressure in the lab, the freeze point and internal pressure data from the hygrometer allow for accurate calculation of the vapor pressure in the TAG oxidation chamber. The partial pressures of water and hydrogen in the reaction were varied by adjusting the water bath temperature and the flow rates on each gas line.

The TAG 16/18 thermogravimetric analyzer is a very sensitive, highly stable microbalance instrument with symmetrical design. Two identical objects (the graphite sample and an inert quartz reference) are suspended by platinum rods and dangle freely into a pair of identical vertical furnace. Buoyancy effects which usually perturb gravimetric measurements at high temperature are much reduced in the symmetrical design. Data collection (sample temperature and weight) was performed by the CALISTO software supplied with the TAG (accuracy of  $\pm 0.1$  °C and  $\pm 0.10$   $\mu$ g).

The DCS 350 mass spectrometer was intermittently used for analysis of gas composition. Collection and analysis of mass spectra was done by the QUADERA software delivered with the equipment. Some technical issues with this equipment precluded its continuous use. However, when the mass spectrometer became available later in the experiments, it was used to confirm that other oxidizing impurities (O<sub>2</sub>, CO<sub>2</sub>) were absent from the reaction chamber of the thermoanalyzer.

The steps taken for accurate calibration of all sensors of the oxidation equipment were detailed in a previous report [23]. Preliminary tests confirmed that the hygrometer responds correctly to flow rate changes of dry and moist He lines and changes of water bath temperature. The hygrometer's operation is based on fundamental thermodynamic properties of water vapors. This instrument is intrinsically capable of long-term accurate and stable operation. The instrument's performance was annually checked by the manufacturer against NIST-certified standards. The equations used for converting mirror's temperature readings into water vapor pressure in the hygrometer chamber were as follows:

$$P_{H_2O} = 6.1121 \exp [(18.678 - T_{DP} / 234.5) (T_{DP} / (T_{DP} + 257.14))] \quad \text{for } T_{DP} > 0 \text{ } ^\circ\text{C} \quad (2a)$$

$$P_{H_2O} = 6.1115 \exp [(23.036 - T_{DP} / 333.7) (T_{DP} / (T_{DP} + 279.82))] \quad \text{for } T_{DP} < 0 \text{ } ^\circ\text{C} \quad (2b)$$

where  $P_{H_2O}$  is water pressure in mbar and  $T_{DP}$  is the dew point (or frost point) temperature in °C measured by the hygrometer. The actual water vapor pressure in the TAG oxidation chamber was calculated by correcting  $P_{H_2O}$  from Eq. (2b) by the  $P_{bar}/P_{hygr}$  factor, where  $P_{bar}$  is the current barometric pressure in the lab and  $P_{hygr}$  is the total pressure inside the hygrometer cell:

$$P_{H_2O} (oxidation) = P_{H_2O} \frac{P_{bar}}{P_{hygr}} \quad (3)$$

This result was cross-checked against mass balance calculations using actual flow rates for each gas line and calculated water vapor pressures at the temperature of the water bath. Although the agreement between water vapor pressure values based on hygrometer readings and calculated from flow rates and mass balance was good [23], the values calculated from Eqs. (2b) and (3) and direct hygrometer readings and were preferred because they were affected by lesser errors.

### 3. MATERIALS

#### 3.1 GRAPHITE SAMPLES

A billet of NBG-17 graphite purchased for the NGNP program was cut according to the diagram in Figure 2 [24]. The billet retained for material characterization at ORNL was cut as shown in Figure 3 [22]. The sub-section labeled Section-A was further used to machine specimen for oxidation by water.

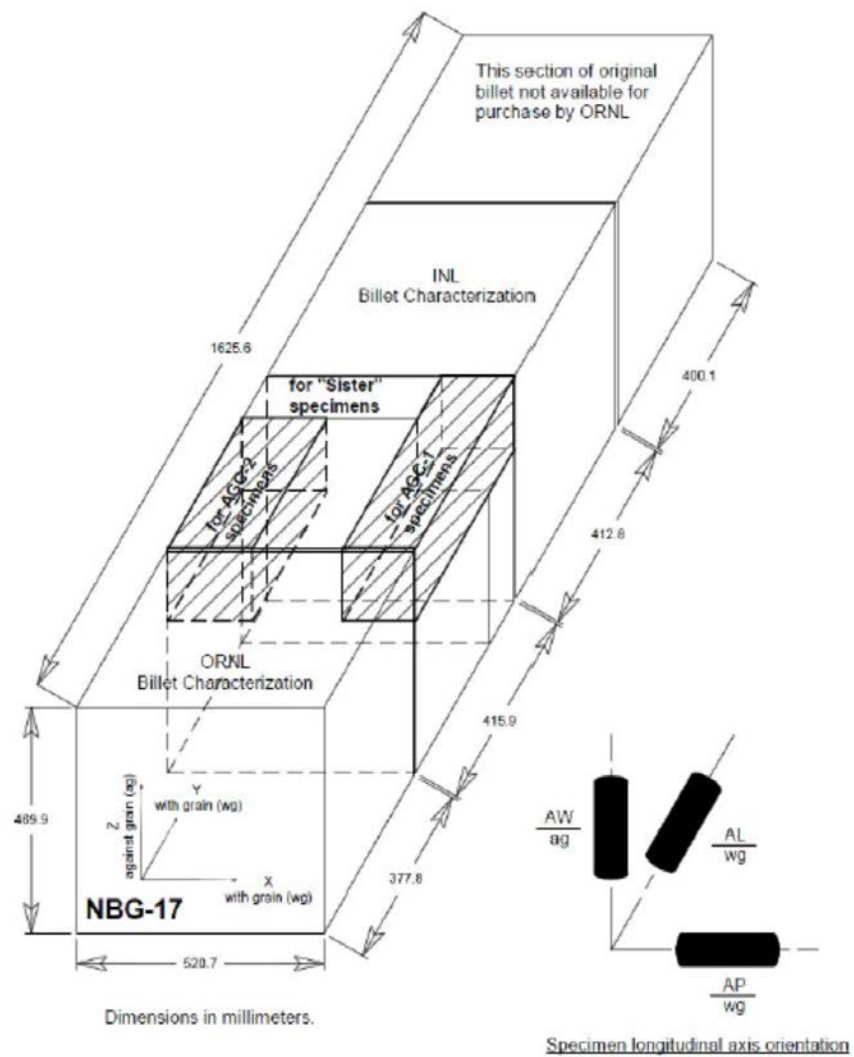


Figure 2: Cutting diagram of NBG-17 billet [24].

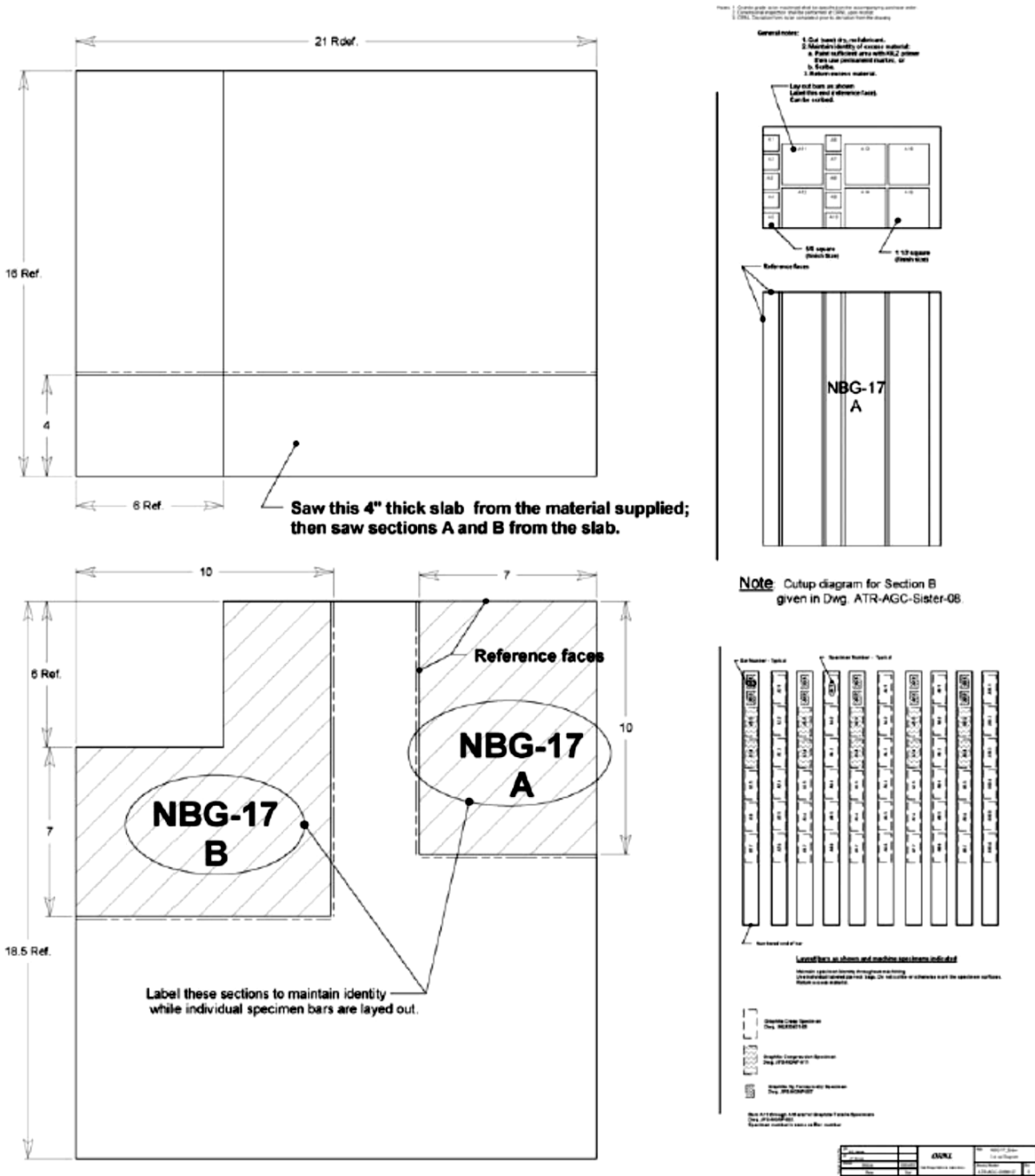
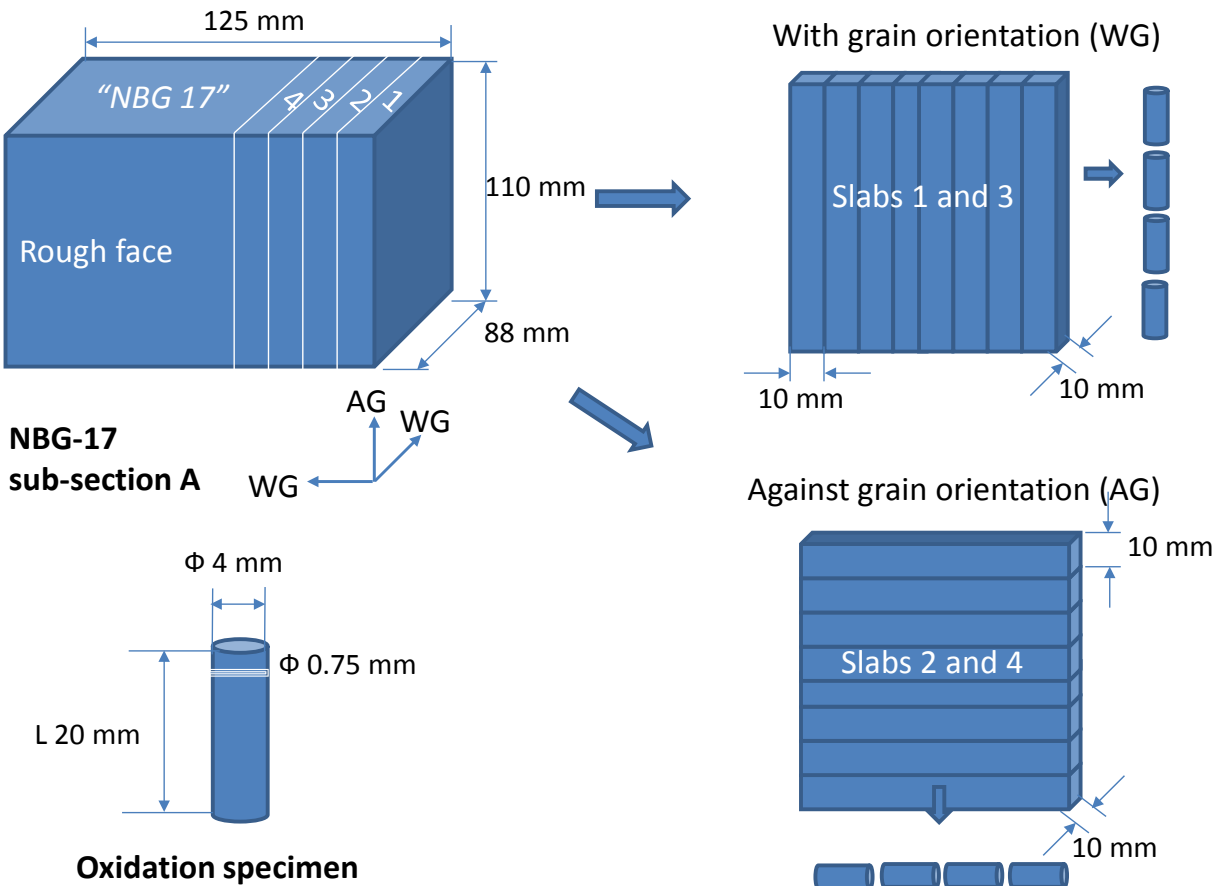


Figure 3: Cutting diagram of the ORNL sub-section of NBG-17 billet [22].

All NBG-17 specimens used in this study had identical shapes and dimensions: right cylinders, 20 mm long  $\times$  4 mm diameter. They were cut from subsection A of the NBG-17 billet with two different orientations: against grain (AG) and with grain (WG). The specimen extraction plan is shown in Figure 4. All specimens were machined in dry conditions (no lubricants) and using only non-metal containing cutting tools.



**Figure 4:** Specimen extraction scheme for NBG-17 oxidation by water.

Graphite anisotropy is usually expressed as the ratio of coefficients of thermal expansion in the AG and WG direction [22]. Compared with the extruded PCEA graphite, the vibrationally-molded grade NBG-17 is more isotropic; therefore, the specimen orientation in the billet is not expected to cause significant property variations. This was confirmed by measurements of oxidation rates of AG and WG oriented specimens performed early in the research program. Data analysis did not show differences that could be confidently attributed to the anisotropy of structural properties. Based on that analysis, in later experiments the orientation (AW or WG) of specimens was disregarded. Specimens with both orientations were randomly used to obtain a non-biased snapshot of mean graphite properties.

### 3.2 GASES

Ultra-high purity (UHP) helium was procured from Air Liquide in batches of 16 interconnected pressurized gas cylinders. Each batch was accompanied by lot analysis certifying that the gas corresponds to quality specifications:

		<u>Specification</u>	<u>Analysis (several batches)</u>
Major component:	Helium	99.9990%	99.9999%
Impurities	Moisture	< 3ppm	0.2–0.3 ppm
	Oxygen	< 2 ppm	0.8–1.7 ppm
	Hydrocarbons	<0.5 ppm	< 0.1 ppm

Hydrogen was delivered from a compressed gas cylinder containing certified mixture of 1 % H<sub>2</sub> in UHP helium (Air Liquide). The certificate of accuracy accompanying the gas provides the following information:

<u>Component name</u>	<u>Requested concentration</u>	<u>Certified concentration</u>	<u>Blend tolerance (+/-)</u>	<u>Certified accuracy</u>
Hydrogen	1 mole %	1.00 mole %	± 0.0 %	± 2.00 %
Helium	balance	balance		

Water used for adding moisture to the helium line through the saturator bubbler was Plasma Grade Water (Fisher Scientific) with certified analysis of metal impurities (most ions < 0.1–1 ppt).

For supplemental protection of gas line purity, moisture traps and oxygen traps were used on the dry He and H<sub>2</sub>/He mixture lines. The oxygen traps (Oxy-purge N from Fisher Scientific) are rated to remove oxygen from inert gases down to the ppb level (or  $\sim 10^{-2}$  Pa when delivered at atmospheric pressure). The moisture traps (Drierite, from Fisher Scientific) are rated for drying the air up to a frost point of  $-73$  °C at a flow rate of 200 L/h. The corresponding water vapor pressure is 0.2 Pa. Our experiment used a lower flow rate (1.5 L/min or 90 L/h) so that the efficiency of the moisture trap was higher. On the other hand, the residual moisture in the UHP He, according to specifications and analysis results, is in the range of 0.02–0.03 Pa (when delivered at atmospheric pressure). This is much lower than the lowest end-of-scale sensitivity limit for the hygrometer, which cannot measure frost points below about  $-55$  °C (corresponding to 2 Pa water partial pressure). It is reasonable to suspect that hygrometer readings were inaccurate at the lowest end scale (below about 5 Pa H<sub>2</sub>O) and the actual water pressures were lower.

## 4. PROCEDURE

### 4.1 TEST CONDITIONS

Graphite oxidation by water is extremely slow in normal operating conditions and the rates cannot be measured. The solution is to use accelerated oxidation tests so that the rates can be measured. Accelerated tests were designed to mimic as close as possible the normal operating conditions. The variables were as follow:

- Temperature range: 800 to 1100 °C
- Water pressure: 3 to 1000 Pa
- Hydrogen pressure: 0 to 40 Pa
- Total flow rate 1.5 L/min
- Linear flow velocity 8 cm/s
- In-situ outgassing temperature before tests 1200 °C
- Duration of in-situ outgassing before tests 1–2 h

### 4.2 PREPARATION OF SPECIMENS BEFORE TESTS

Before tests, each graphite specimen was cleaned for 10 minutes by sonication in acetone and dried in air at 110 °C. Cleaned specimens were handled only with cotton gloves or plastic tweezers.

Physical measurements (weight and dimensions) were taken on each cleaned specimen just before the tests, according to ASTM C559-90 [25]. All physical measurement data are provided in Annex 1.

### 4.3 OXIDATION TEST PROCEDURE

After physical measurements were taken, the specimens were attached with platinum wires to the sample arm of the microgravimetric balance in the TAG and were centered in the furnace. A similar volume quartz reference sample was attached to the reference arm of the TAG, and the furnace was raised to its working position.

The initial weight of each specimen was entered in the test information file and served as the reference weight for weight loss calculations.

The procedure used for most tests consisted of the following steps:

1. Turn on and start simultaneously the LabView software for gas flow control and water bath temperature, the pre-programmed procedure for thermogravimetric analysis (CALISTO) and (in some cases) the mass spectrometer procedure (QUADERA).
2. Flow 1.5 L/min dry UHP He for 20 min at room temperature.
3. Ramp temperature at 10 °C/min to 1200 °C.
4. Outgas the specimen at 1200 °C for 1 or 2 h while flowing 1.5 L/min dry UHP He.
5. Lower temperature at 10 °C/min to the first test temperature while flowing 1.5 L/min dry UHP He.
6. Introduce water (or water and hydrogen mixture) in the UHP He stream at total flow rate of 1.5 L/min and adjust composition to the target partial pressures of H<sub>2</sub>O and H<sub>2</sub>.

7. Execute the preselected time- temperature- gas composition program consisting of dwelling segments (2-6 hours) at constant conditions ( $T$ ,  $P_{\text{H}_2\text{O}}$ , and  $P_{\text{H}_2}$ ) separated by transitory conditions (temperature ramps at 10 °C/min or variations of  $P_{\text{H}_2\text{O}}$  and  $P_{\text{H}_2}$ ) while maintaining a total flow rate of 1.5 L/min He with added H<sub>2</sub>O (and H<sub>2</sub> in some experiments).
8. Lower the temperature (25 °C/min) to 25 °C after last segment while flowing 1.5 L/min gas with the last composition.
9. Continue flowing 1.5 L/min gas with previous composition for another 10 min and end the test.

The total duration of most tests was approximately 24 h. Other tests were purposely designed to measure the effect of gas composition at constant temperature. These tests were longer (up to 120 h). The gas composition was varied by remote computer control of dry He, moist He, and the H<sub>2</sub>/He mixture.

Some tests at low temperature and low water vapor pressure were affected by the inadvertent oxidation of suspension rods made from a Ni-Cr alloy. This alloy is sensitive to surface oxidation when exposed to water vapor at 800-900 °C. Oxidation caused a weight increase (not decrease, as expected for graphite gasification), which resulted in “negative” rate values. These parasitic effects were particularly significant in conditions in which the oxidation rates were slow (low temperatures, low water vapor pressures). Oxidized rods were recognized by the discoloration that replaced the metallic shine on their surfaces. The problem was corrected by replacing the Ni-Cr rods with platinum rods.

After recalibration of the mass spectrometer and replacement of the ion source, several tests were performed in carefully controlled conditions with mass spectrometric analysis of the gas composition. The purpose of these tests was to obtain accurate measurements of very slow oxidation rates. The purity of the gas was controlled by evacuating the whole system, followed by controlled helium introduction, with simultaneous monitoring of gas composition. This procedure led to very clean gas streams, free of residual oxygen and nitrogen, and very low amounts of moisture. Several measurements of slow oxidation rates performed in these conditions proved that the weight increases previously observed were an experimental error. Consequently, all data showing “negative oxidation rates” were discarded before the final analysis of results.

#### 4.4 SPECIMEN CHARACTERIZATION AND DATA SAVING AFTER TESTS

Each oxidized specimen was collected after tests and physical measurements were repeated. All results are presented in Annex 1. Oxidized specimens were labeled and stored in plastic bags.

The following data were saved after each test:

- LabView data in text format. Data contain time, flow rates of MF1, MF2, and MF3, dew point and internal pressure from hygrometer, water bath temperature, and ambient conditions in the lab (temperature, humidity, and barometric pressure).
- TAG data processed by CALISTO software. Analysis comprised calculation of weight losses during each segment at constant temperature from the TG curve, calculation of instantaneous weight loss changes from the DTG curve, and graphic representation of data. All data were saved both in graphic and Excel format. See Annex 2 for all oxidation rate data.
- QUADERA data from mass spectrometer. These data were saved (when available) in graphic and ASCII format.
- Excel data files with operator’s notes during tests and screen prints of LabView application at the end of experiments, showing plots of hygrometer readings and various flow controller data collected in real time.

### 4.5 DATA REDUCTION

Instantaneous values of water vapor pressure inside the oxidation furnace were calculated using Eqs. (2b) and (3). The average values calculated for each segment of constant conditions were then correlated with the corresponding average oxidation rates. For each segment, the oxidation rates were calculated as  $\Delta w / \Delta t$ , where  $\Delta w$  is the weight variation and  $\Delta t$  is the corresponding duration of each constant conditions segment on TG curves. The absolute weights corresponding to each segment were calculated from the initial specimen weight, the weight loss during high temperature outgassing, and the weight variations in previous segments. Figure 5 shows an example of processed data in a run at constant water vapor pressure and variable temperature. Figure 6 shows an example of a run at constant temperature and variable water vapor pressure and hydrogen pressure.

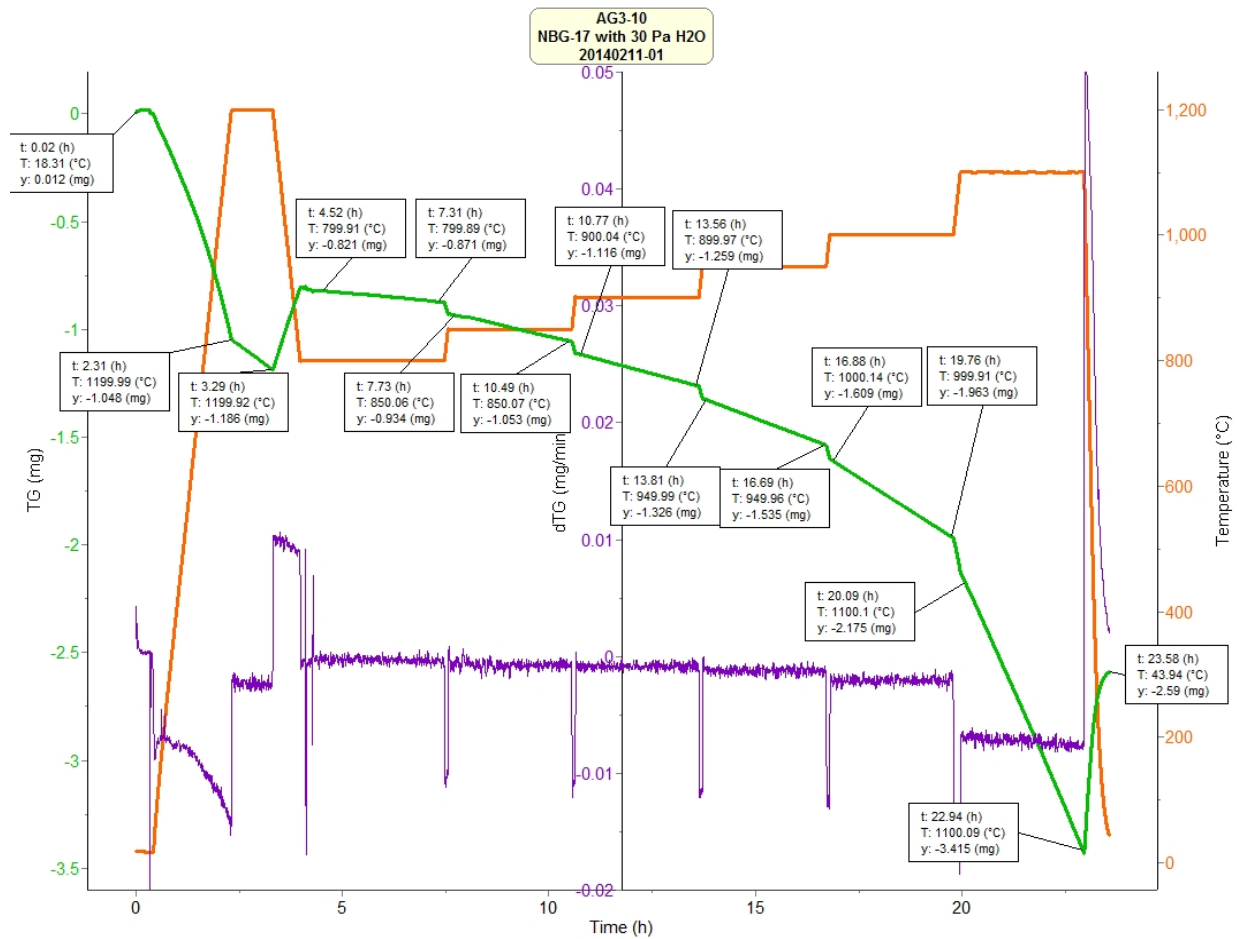


**Figure 5:** Example of processed TG data recorded in a 24 hour long run where water pressure was kept constant (30 Pa) and the temperature was increased from 800 to 1100 °C (red = temperature; green = TG; purple = DTG).

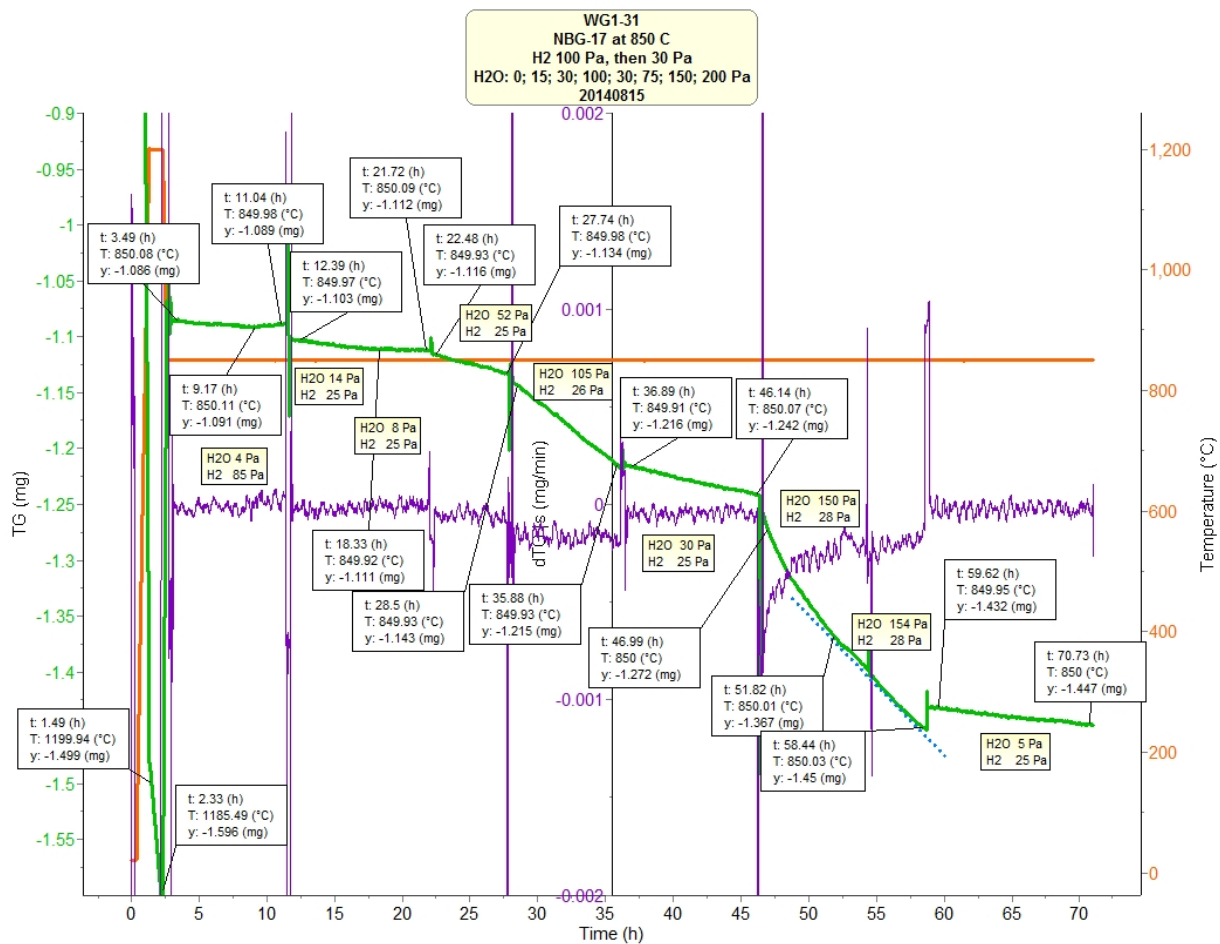


**Figure 6:** Example of processed TG data recorded in a 72 hour long run where temperature was kept constant (850 °C) and water vapor pressure and hydrogen pressure were varied (red = temperature; green = TG; purple = DTG).

Based on prior experience [23], no attempts were made to correct the variation of oxidation rates caused by graphite “burn-off”.<sup>(\*)</sup> In the model proposed by Su and Perlmutter [26], the increase of oxidation rates with time (or burn-off) is attributed to development of new porosity during extensive oxidation, which is modeled by introducing a graphite-specific structural parameter. While this correction is significant at high oxidation levels in air [27,28] it is not expected to be important in the present experiments where the oxidation level was always < 2 %. Prior attempts [10,23] to determine the structural factor for graphite PCEA showed that the empirically found factors that would flatten the weight change profiles were not constant. Rather than introducing another empirical variable, which would randomly affect the oxidation rates, it was decided not to use the burn-off correction for low levels of oxidative weight loss.

<sup>(\*)</sup> The expression “burn-off” is used here to keep consistent with the cited publication by Su and Perlmutter. In reality, it is a scientifically demonstrated fact that graphite does not burn.

## 5. DATA ANALYSIS

### 5.1. LANGMUIR-HINSHELWOOD KINETIC MODEL

The gasification reaction between carbon (graphite) and water becomes thermodynamically possible at temperatures above  $\sim 700$  °C:



It has been documented for a long time [11,12,13,14] that graphite oxidation by water follows a complicated mechanism, known as the Langmuir-Hinshelwood (L-H) mechanism, described by the following reaction rate expression:

$$Rate = \frac{k_1 P_{H_2O}}{1 + k_2 (P_{H_2})^n + k_3 P_{H_2O}} \quad , \quad (5)$$

where rate constants  $k_i$  obey an Arrhenius type temperature dependence with two parameters, the pre-exponential (or frequency) factor  $A_i$  and the activation energy  $E_i$ :

$$k_i = A_i e^{-\frac{E_i}{RT}} \quad , \quad (6)$$

where  $R$  is the universal gas constant and  $T$  is the absolute temperature.

The mechanism of elementary reaction steps for gasification by water is still debated. In the scheme proposed by Gatsby [11,12], the surface sites on graphite are blocked by molecularly adsorbed hydrogen ( $H_2$ ); in this case the exponent from Eq. (5) should have the value  $n = 1$ . This mechanism was accepted by Burnette et al. at General Atomic Company, who provided numerical values of all kinetic constants in Eqs. (5) and (6) for oxidation of graphite H-451 by moisture [8]. However, more recent arguments [29] supported by modeling of carbon-hydrogen surface interactions [30,31] suggest a mechanism whereby the blocking of surface sites is caused by atomic H, not molecular  $H_2$ . This leads to  $n = 0.5$  in Eq. (5). Previous analysis of accelerated oxidation tests by moisture of PCEA graphite used  $n = 0.5$  [10,23]. The same assumption is used in the present analysis.

In summary, the goal of this study is determination of the six numerical parameters  $A_i$  and  $E_i$  ( $i = 1, 2, 3$ ) in the explicit rate equation obtained by combining eqs. (5) and (6):

$$Rate = \frac{A_1 \exp\left(-\frac{E_1}{RT}\right) P_{H_2O}}{1 + A_2 \exp\left(-\frac{E_2}{RT}\right) (P_{H_2})^{0.5} + A_3 \exp\left(-\frac{E_3}{RT}\right) P_{H_2O}} \quad (7)$$

Knowledge of these six parameters will allow predictions of local oxidation rates of NBG-17 graphite at any given temperature, water vapor partial pressure, and hydrogen partial pressure. A similar modeling

task was accomplished by Richards [32] using the parameters for graphite H-451 from the General Atomics study cited earlier [8].

Finding the numerical values for the L-H parameters in Eq. (7) is complicated by several factors: (i) the equation is highly nonlinear in pressure; (ii) it has triple exponential dependence of oxidation rates by the reciprocal of absolute temperature; and (iii) its parameters are highly correlated through the Arrhenius relationship, Eq. (6), that links preexponential terms  $A_i$  with activation energies  $E_i$ . Moreover, the significance of rate constants  $k_i$  in gas-solid reactions is difficult to ascertain in the absence of a detailed mechanism in the chain of elementary step reactions that compose the overall gasification reaction. The pathway of the oxidation reaction may change with the change in external conditions, because the weight of various elementary reaction steps may be affected by temperature or gas composition. Unlike in the formal kinetics of gas-phase reactions, the presence of porosity, which introduces transport factors in the kinetic equation, complicates the problem even more. For that reason, all  $A_i$  and  $E_i$  found by fitting should be regarded as apparent (or mechanism-conditioned) parameters. It is not uncommon for apparent rate constants to have unusual variations. There are examples in the literature on graphite oxidation that show *negative* values for some apparent activation energies [12], which is quite unusual in the formal chemical kinetics. Such results were also found in the previous study on PCEA oxidation [10,23] and in the current study as well.

## 5.2 DETERMINATION OF KINETIC PARAMETERS

Table A-1 (in the Annex) lists physical properties of 49 NBG-17 specimens analyzed over 52 runs. A total of 302 experimental observations were initially considered. Of these, 33 observations were rejected. Of them, 18 observations returned negative oxidation rates at 800 and 850 °C (as explained earlier) and 15 measurements were clearly in error compared with the rest of the data. These observations were identified as extreme outliers, based on an empirical response surface model. The rest of the 269 valid observations (89 % of the total experimental data) were retained for further analysis. Table A-2 (in the Annex) lists the parameters of all observations (valid and rejected).

Data analysis and statistical treatment using the maximum likelihood estimate (MLE) approach was performed by Professor Robert Mee at the University of Tennessee, Knoxville, TN. When applied to a set of data in combination with a statistical model assumed for a particular situation, MLE provides standard errors for the estimates and correlations between the estimates. That is, given data from many runs at different conditions, the MLE approach is to simultaneously estimate the parameters that best represent the data. This is essential for understanding the uncertainty in the parameter estimates.

After the data were validated as explained, the SAS Institute procedure NLMIXED was used to fit the six parameters of the L-H model. The rate equation, Eq. (7), was rewritten in logarithmic form as follows:

$$\ln(\text{Rate}) = \ln(P_{H2O}) + a_1 + \frac{b_1}{T} - \ln \left[ 1 + P_{H2O} \exp \left( a_3 + \frac{b_3}{T} \right) \right] + \varepsilon + \delta \quad (8)$$

where  $a_i = \ln A_i$  and  $b_i = E_i/R$ . Taking  $\ln(\text{Rate})$  as the response variable, it was assumed that there were two additive sources of random errors, normally distributed:  $\varepsilon$  is the error associated with each individual measurement ( $n = 269$ ) and  $\delta$  is the error associated with each separate run ( $m = 52$ ). The variability represented by  $\delta$  accounts for any material heterogeneity, since a fresh graphite specimen was used in each run (with the exception only of specimen 49 which was used on days 49–52).

A nonlinear mixed model represented by Eq. (8) was assumed. The SAS procedure PROC NLMIXED maximizes an approximation in the likelihood function for the six L-H parameters and the two variance components. PROC MLMIXED also furnishes an approximate 95 % confidence interval for

each parameter, assuming that the model is correct. The model can also furnish confidence intervals for the average  $\ln(\text{Rate})$  for samples of this graphite at any given combination of experimental inputs.

Table A3 (in Annex) shows the fitted parameters provided by SAS along with the standard errors and 95 % confidence intervals. These results were obtained by employing all 269 valid observations over the full range of temperatures investigated (800–1100 °C). The confidence intervals for the preexponential factors  $A_i$  were calculated by taking the exponential of the endpoints of the corresponding confidence intervals for  $a_i = \ln(A_i)$ ; this explains why the ML estimate for each  $A_i$  is not in the middle of the corresponding confidence interval. The standard errors associated with the activation energies  $E_2$  and  $E_3$  are respectively 20 % and 26 % of the estimated values. However, the error affecting the activation energy  $E_1$  is twice as large (47 %).

The estimates of corresponding parameters of the L-H model are reported in Table 1. Figures 7 and 8 compare measured oxidation rates with predicted rates using these estimates. The two figures detail the effect of temperature and water vapor pressure on the oxidation rates. Figure 7 shows measured data and predicted trends for oxidation caused by water vapor alone (no hydrogen). Data in this figure show a very small temperature effect on oxidation rates at low water vapor pressures. Indeed, the isothermal plots of predicted rates are well separated at high  $P_{\text{H}_2\text{O}}$  and congregate closely toward low  $P_{\text{H}_2\text{O}}$ . This is the consequence of the low value of activation energy  $E_1 = 61.5$  kJ/mol found for graphite NBG-17.<sup>(†)</sup> In contrast, Fig. 8 shows that adding 26 Pa of hydrogen to the oxidation gas causes strong inhibition of oxidation rates. The rates predicted in the presence of  $\text{H}_2$  show almost parallel trends and spread over several orders of magnitude. Particularly, when  $P_{\text{H}_2} \geq P_{\text{H}_2\text{O}}$ , the inhibition by hydrogen causes a hundred times drop in oxidation rates (compare rates at 3 Pa  $\text{H}_2\text{O}$  in the presence of 26 Pa  $\text{H}_2$  in Fig. 8 and without  $\text{H}_2$  in Fig. 7).

**Table 1.** L-H fitted parameters using all valid 286 observations

$A_1 = 3.85 \times 10^{-6} \text{ Pa}^{-1} \text{ s}^{-1}$	$E_1 = 61.5 \text{ kJ/mol}$
$A_2 = 4.00 \times 10^{-8} \text{ Pa}^{-0.5}$	$E_2 = -186.7 \text{ kJ/mol}$
$A_3 = 5.79 \times 10^{-7} \text{ Pa}^{-1}$	$E_3 = -122.9 \text{ kJ/mol}$
$n = 0.5$	

<sup>(†)</sup> The activation energy  $E_1$  reported for the first L-H rate constant  $k_1$  is higher for H-451 (274 kJ/mol) and PCEA (208 kJ/mol) graphite grades [8,23].

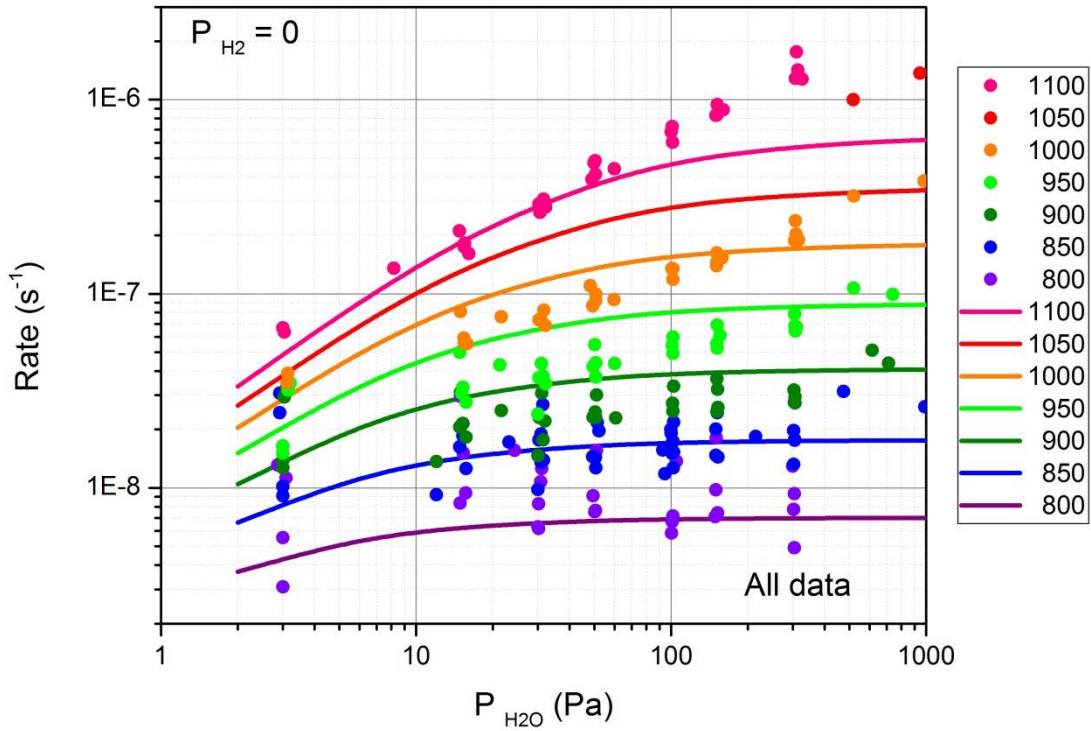


**Figure 7:** Oxidation rates predicted with parameters in Table 1 versus observed rates at  $P_{H_2}=0$ .

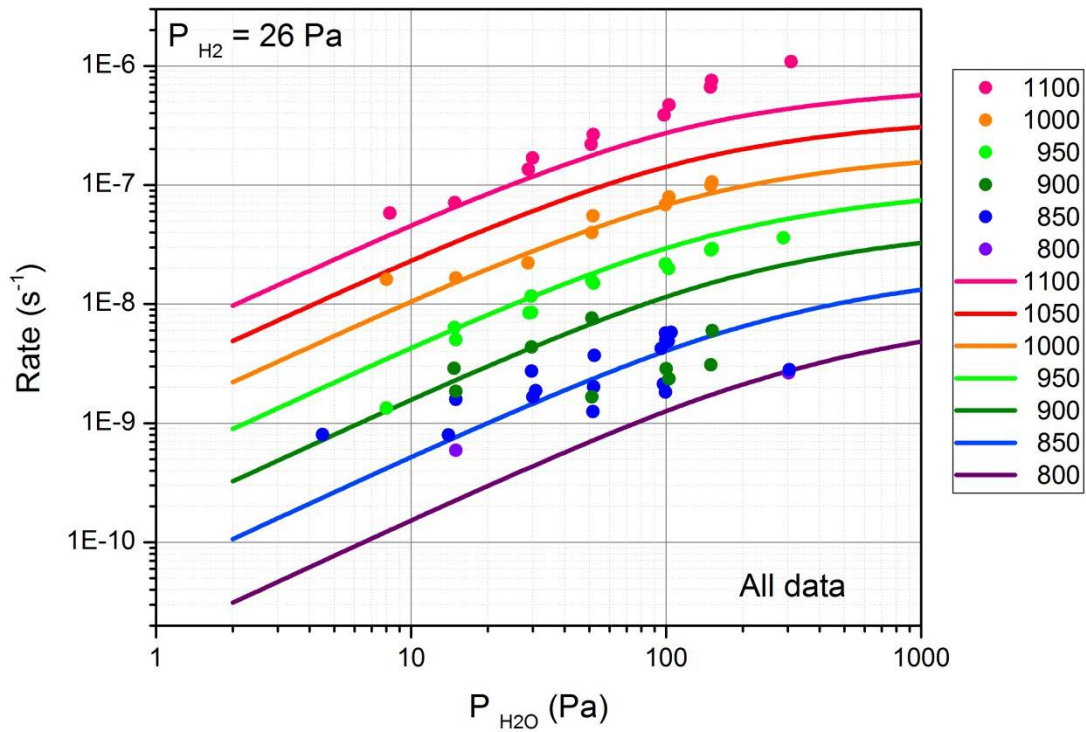


**Figure 8:** Oxidation rates predicted with parameters in Table 1 versus observed rates at  $P_{H_2}=26$  Pa.

Figure 9 shows a direct comparison between all valid rate measurements and the corresponding rates predicted using parameters from Table 1. The double logarithmic scale was selected to compensate for the large variation (three orders of magnitude) of all data. If predicted rates were identical to the observed values, the plot would be a straight line with the unity slope, the residual sum of squares would be zero, and the correlation coefficient would be one. In fact, a linear fit with slope 1 applied to all 269 valid data points in Fig. 9 indicates a reasonable correlation between predicted and measured rates (adjusted  $R^2 = 0.899$ ; residual sum of squares = 12.6). However, a second degree polynomial gives a better fit (adjusted  $R^2 = 0.911$ ; residual sum of squares = 11.0). In fact, the lack of fit of rates higher than  $10^{-7} \text{ s}^{-1}$  is easily detected.

Although the parameters in Table 1 appear to provide a reasonable fitting of experimental data over the range of temperatures and pressures investigated, Figs. 7 and 8 show also some evidence of lack of fit. For example, data at 1000 and 1100 °C and  $P_{\text{H}_2\text{O}} > 50 \text{ Pa}$  are clearly underestimated by the fit based on all 269 valid rate measurements. One concludes that the L-H model with the best fit parameters from Table 1 underestimates fast oxidation rates.

In an attempt to refine the model, the rate data were split in two groups: low temperature data (191 observables between 800 and 950 °C) and high temperature data (166 observables between 900 and 1100 °C). The groups were fitted separately, but the statistical parameters (reported in Table A3) did not improve the fit sufficiently to justify using two separate models. Moreover, fitting the L-H model for the low temperature group produced negative values of all three activation energies, which is inconsistent with physical models.

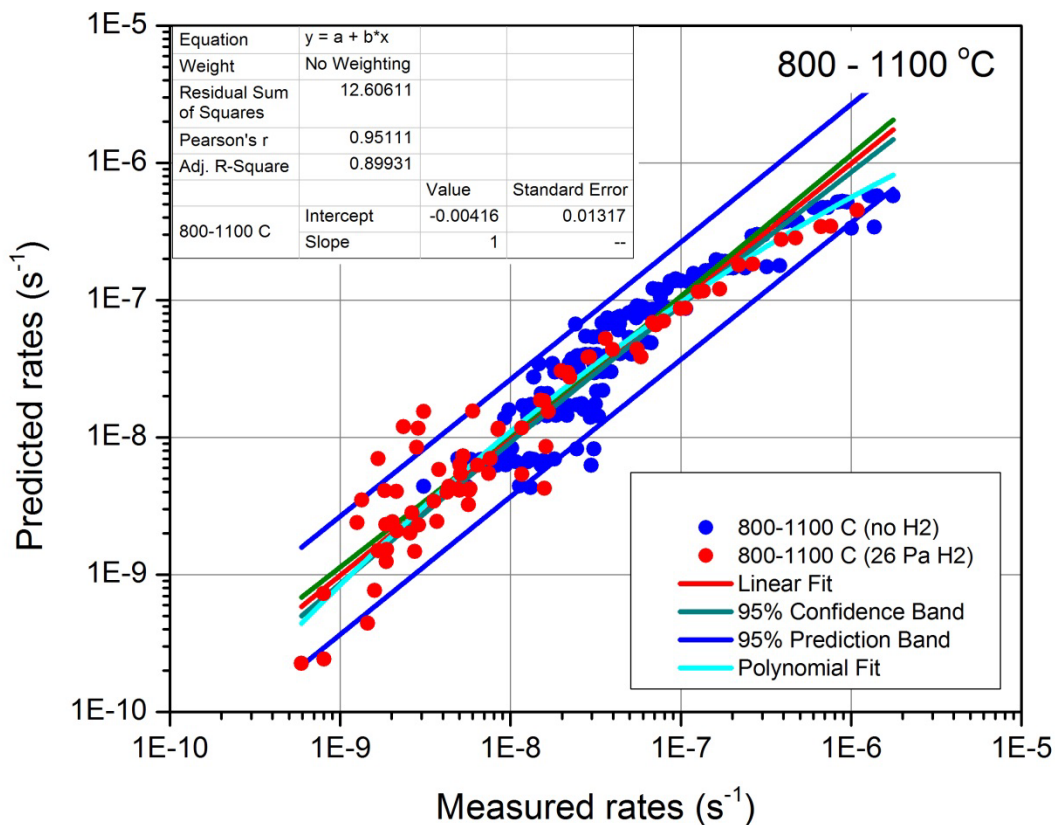


**Figure 9:** Comparison between oxidation rates predicted with parameters in Table 1 and actual measured rates. The rates observed with and without  $\text{H}_2$  in the oxidation gas are marked by differently colored symbols.

## 6. DISCUSSION OF RESULTS

Fitting the L-H model and finding the kinetic parameters in Eq. (7) is known to pose theoretical difficulties because of the multiple nonlinear form of the equation and the strong correlation between parameters. Ideally, obtaining data over a broad interval of  $P_{\text{H}_2\text{O}}$ ,  $P_{\text{H}_2}$ , and  $T$  may improve the accuracy of results. However, this is not possible from the experimental point of view. The temperature range is limited at both ends. Below 700 °C oxidation of graphite by water is not thermodynamically possible; even at 800 °C the rates are too slow for accurate determination. On the other hand, the rates are very fast at 1100 °C, and oxidation reactions may become perturbed by slow diffusion of the oxidant. The useful range for measurements is between 800-850 and 1100 °C .

Despite these difficulties, oxidation rate measurements of two grades of nuclear graphite, PCEA [10,23] and NBG-17 (this work), were shown to obey the L-H model within some reasonable limits. As in the previous work with PCEA graphite, not all oxidation rate data measured for graphite NBG-17 were validated for final analysis of results. Less than 10 % of data identified as extreme outliers had to be rejected for the reasons stated in section 5.

With that correction, the oxidation rate values predicted by the L-H model were reasonably well correlated with the experimental measurements, as shown in Fig. 9. The quality of fit for NBG-17 graphite in this work is comparable to that reported previously [10] for PCEA graphite (adjusted correlation coefficients  $R^2$  is 0.9067 for 190 data points with PCEA and 0.8993 for 269 data points with NBG-17; Pearson's  $r$  parameter is 0.95797 for PCEA and 0.95111 for NBG-17).

**Table 2:** Summary of L-H parameters for three nuclear graphites

	$A_1$ Pa <sup>-1</sup> s <sup>-1</sup>	$E_1$ kJ/mol	$A_2$ Pa <sup>-0.5</sup>	$E_2$ kJ/mol	$A_3$ Pa <sup>-1</sup>	$E_3$ kJ/mol
<b>NBG-17 graphite (this work)</b>						
	<b><math>3.85 \times 10^{-6}</math></b>	<b>61.5</b>	<b><math>4.00 \times 10^{-8}</math></b>	<b>-186.6</b>	<b><math>5.79 \times 10^{-7}</math></b>	<b>-122.8</b>
95% confidence intervals [lower; upper]	[ $2.6 \times 10^{-6}$ ; $5.7 \times 10^{-5}$ ]	[32.4; 90.6]	[ $1.1 \times 10^{-9}$ ; $1.5 \times 10^6$ ]	[-149.2; -224.0]	[ $2.7 \times 10^{-8}$ ; $1.2 \times 10^{-5}$ ]	[-90.8; -155.0]
<b>PCEA graphite [10]</b>						
	<b>0.69</b>	<b>200.9</b>	<b><math>8.1 \times 10^{10}</math></b>	<b>310.6</b>	<b><math>4.6 \times 10^{-4}</math></b>	<b>-36.6</b>
95% confidence intervals [lower; upper]	[0.06; 8.34]	[175; 227]	[ $9.1 \times 10^{-14}$ ; $7.1 \times 10^{34}$ ]	[-321; 942]	[ $9.8 \times 10^{-6}$ ; $2.1 \times 10^{-2}$ ]	[-76; 3.3]
<b>H-451 graphite [8]</b>						
0-300 Pa H <sub>2</sub> O	<b>2000</b>	<b>274</b>	<b>1100</b>	<b>74.6</b>	<b>200</b>	<b>95.8</b>
300-3500 Pa H <sub>2</sub> O	<b>0.11</b>	<b>195</b>	<b><math>7.9 \times 10^{-8}</math></b>	<b>119.7</b>	<b><math>1.3 \times 10^{-9}</math></b>	<b>131.4</b>
0-3500 Pa H <sub>2</sub> O	<b>900</b>	<b>274</b>	<b><math>1.1 \times 10^2</math></b>	<b>74.66</b>	<b>30</b>	<b>95.85</b>

Table 2 compares the L-H parameters for slow oxidation by water of three graphite grades for which detailed kinetic analysis is now available: H-451 [8], PCEA [10] and NBG-17 (this work). The parameters differ considerably between graphite grades. This finding does not come as a surprise: it is known that fitting of a complicated nonlinear equation such as the L-H model may produce multiple sets of local optimal parameters, depending on the initial “guess” introduced in the fitting algorithm. The problem is further complicated by the inherent experimental errors and the likely inhomogeneity of the material [33]. In addition, the use of linearization methods with non-linear models may provide point estimates of parameters, but their exact value remains uncertain because of the assumption that the model is linear in the neighborhood of these point estimates. This is certainly the case with the results reported for graphite H-451, where the L-H parameters were obtained by a successive linearization algorithm. In this method, the errors from successive linearization steps compound with one another and result in greater uncertainty of the parameters found. Analysis of PCEA and NBG-17 oxidation data was carried out using the more powerful MLE approach. In this statistical method, all parameters are fitted simultaneously on a large set of experimental observations, and the final selection is based on the maximum likelihood with the observables. Inherent to this approach is the assumption that the original model, as expressed by Eq. (7), is valid over the whole range of pressures and temperatures. The stability of the model is based, in turn, on the tacit assumption that each individual elementary reaction step of the overall complex kinetic mechanism does not change with pressure and temperature. This is difficult to justify, especially for gas-solid reactions that might be affected by significant diffusion perturbations as the external conditions vary. Nonetheless, the fact that a multitude of experimental oxidation rate data, spanning three orders of magnitude, can be reasonably reproduced by the L-H model with a set of six parameters justifies, in general, the applicability of this model for graphite oxidation by water. This is the best that can be done at this time. In the near future, when more information becomes available for graphite grades with significant differences in microstructure, a fresh look at the limits of the L-H model will be worthwhile. A more flexible approach, although pragmatic and perhaps remote from the assumptions of the L-H model, might allow more accurate prediction of long term graphite oxidation behavior.

## 7. CONCLUSION AND FUTURE WORK

This kinetic study of oxidation by water of nuclear graphite NBG-17 follows a similar study completed in 2013 on graphite PCEA [10,23]. Both graphite grades are possible candidates for manufacturing of components in HTGR systems. A third study of oxidation kinetics by water of graphite IG-110 is now in progress. The purpose of these studies is to obtain material-specific information needed to develop predictive models for evaluation of the extremely slow, but continuous structural damage that will occur in normal operating conditions when graphite components are exposed to very low concentrations of water in the helium coolant. A similar study was performed in 1978 by Velasquez, Hightower, and Burnette for General Atomic Company on the American graphite H-451 [8]. Based on the results for graphite H-451, Richards [32] calculated the density profile under the surface of water-oxidized graphite after prolonged exposure to moisture. He concluded that oxidation of graphite H-451 will be limited to 1–2 mm under the surface of components, provided the water concentration is kept below 0.1 ppm. The model predictions compared favorably with measurements on water-oxidized graphite 2020 (a different grade from H-451) oxidized at 1000 °C in 55 bar of He with 9090 ppm H<sub>2</sub>O and 455 ppm H<sub>2</sub> [32]. The conclusion that graphite oxidation will not affect the reactor integrity during long time HTGR operation was based on this comparison. However, graphite H-451 (used in the Fort St. Vrain reactor) is no longer available. New experimental reactors built in China (HTR-10) and Japan (HTTR) use graphite IG-110. Because no specific information on chronic oxidation by water of this graphite is available, it was assumed that all nuclear graphite grades will reproduce the kinetic behavior of grade H-451 [27,34,35]. Given the known effects of microstructure on the oxidation behavior of various graphite grades [9], the assumption that oxidation rate parameters of graphite grade H-451 can be safely transferred to other graphite grades is questionable.

Investigation of long term oxidation resistance in conditions relevant for normal operation of nuclear reactors is a requirement for qualification of new grades of nuclear graphite for the Advanced Reactor Technology program in the United States. The results obtained with graphites NBG-17 and PCEA show that the L-H model for graphite oxidation by moisture is valid within some reasonable limits. Both graphite grades show deviations from the model at extreme conditions. On the one hand, observed oxidation rates were slower than predicted at low temperatures, low water vapor pressure, and in the presence of hydrogen. On the other hand, they were faster than predicted by the model at high temperatures and high water vapor pressures. Moreover, results for the two graphite grades suggest strongly that the microstructures of particular graphite grades have a strong influence on the kinetic behavior during oxidation by traces of water. This observation corroborates the recent result showing the effect of microstructure on the diffusivity and permeability of graphite for water vapor and helium [18].

This project must continue with examination of the combined effects of kinetic and transport (diffusion) characteristics of graphite grades on oxidant penetration profiles in the subsurface of graphite components. The analysis will use the parameters of the L-H model determined for PCEA and NBG-17 graphites and the water effective diffusivity measurements for the same grades [18]. The expected result is to predict the density profiles of the oxidation layer produced by reactions with water at several temperatures. The predictions will then be compared with the measured oxidation profiles in known experimental conditions. Oxidation profile data for graphite PCEA measured by optical microscopy (at ORNL) and X-ray tomography (at Idaho National Laboratory) are already available. A similar set of measurements should be performed on NBG-17 specimens oxidized by moisture.



## REFERENCES

- 1 M P Kissane, A review of radionuclide behavior in the primary system of a very-high temperature reactor, *Nucl. Eng. Design*, **239** (2009) 3076–3091.
- 2 X Yu, S Yu, Analysis of fuel element matrix graphite corrosion in HTR-PM for normal operating conditions, *Nucl. Eng. Design*, **240** (2010) 738–743.
- 3 E R Corwin, Generation IV Reactors Integrated Materials Technology Program Plan: Focus on Very High Temperature Reactor Materials, ORNL/TM-2008/129 (2008).
- 4 M Fechter, Graphite Oxidation Modeling for a 250 MW Pebble Bed Reactor, ORNL presentation, July 2010.
- 5 B Castle, NGNP Reactor Coolant Chemistry Control Study, INL/EXT-10-10533.
- 6 R N Wright, Kinetics of Gas Reactions and Environmental Degradation in NGNP Helium, INL/EXT-06-11494 .
- 7 T J Clark, R E Woodley, D R de Halas, Gas-graphite systems, in Nuclear Graphite, ed. R E Nightingale, Academic Press (1962), p. 387–444.
- 8 C Velasquez, G Hightower, R Burnette, The Oxidation of H-451 Graphite by Steam. Part 1: Reaction Kinetics, General Atomic Company, GA-A14951 (1978).
- 9 C I Contescu, T Guldán, P Wang, T D Burchell, The effect of microstructure on air oxidation resistance of nuclear graphite, *Carbon*, **50** (2012) 3354–3366.
- 10 C I Contescu, R W Mee, P Wang, A V Romanova, T D Burchell, Oxidation of PCEA nuclear graphite by low water concentrations in helium, *J. Nucl. Mater.*, **453** (2014) 225–232.
- 11 J Gadsby, C N Hinshelwood, K W Sykes, Kinetics of the reactions of steam-carbon system, *Proc. Roy. Soc. (London) A*, **187** (1946) 129–151.
- 12 J Gadsby, F J Long, P Sleightholmm K W Sykes, *Proc. Roy. Soc. (London) A*, **193** (1949) 357.
- 13 L G Overholser, J P Blakely, Oxidation of graphite by low concentrations of water vapor and carbon dioxide in helium, *Carbon*, **2** (1965) 385–394.
- 14 J P Blakely, L G Overholser, Oxidation of ATJ graphite by low concentrations of water vapor and carbon dioxide in helium, *Carbon*, **3** (1965) 269–275.
- 15 R P Wichner, T D Burchell, C I Contescu, Penetration depths and transient oxidation of graphite by oxygen and water vapor, *J. Nucl. Mater.*, **393** (2009) 518–521.
- 16 R P Wichner, T D Burchell, C I Contescu, A Note on the Oxidation of Graphite by O<sub>2</sub> and Moisture, ORNL/TM-2008/230 (2008).
- 17 C I Contescu, Graphite oxidation: Analysis and modeling results, Advanced Materials R&D program review, Advanced Reactor Technologies Program, May 6-8, 2014, Oak Ridge, TN (2014).
- 18 C I Contescu, T D Burchell, Water Vapor Transport in Nuclear Graphite, ORNL/TM-2015/88 (2015).
- 19 P Beghein, G Berlioux, B du Mesnildot, F Hiltmann, M Melin, NBG-17 – An improved graphite grade for HTRs and VHTRs, *Nucl. Eng. Design*, **251** (2012) 146–49.
- 20 J Kane, C Karthik, D P Butt, W E Windes, R Ubic, Microstructural characterization and pore

- structure analysis of nuclear graphite, *J. Nucl. Mater.*, **415** (2011) 189–197.
- 21 Q-K Choi, N-J Kim, E-S Kim, S-H Chi, S-J Park, Oxidation behavior of IG and NBG nuclear graphites, *Nucl. Eng. Design*, **241** (2011) 82–87.
  - 22 T Burchell, S Nunn, J Strizak, M Williams, AGC-1 Sister Specimen Testing Data Report, ORNL/TM-2009/025 (2009).
  - 23 C I Contescu, T D Burchell, R Mee, Accelerated Oxidation Studies of PCEA Nuclear Graphite by Low Concentration of Water and Hydrogen in Helium, ORNL/TM-2013/524 (2013).
  - 24 T Burchell, J Strizak, M Williams, AGC-1 Specimen Pre-irradiation Data Report, ORNL/TM-2010/285 (2010).
  - 25 Standard test method for bulk density by physical measurements of manufactured carbon and graphite articles, ASTM C559-90 (Reapproved 2010).
  - 26 J-L Su, D D Perlmutter, Effect of pore structure on char oxidation kinetics, *AIChE Journal*, **31** (1985) 973–981.
  - 27 X Yu, L Brissonneau, C Bourdeloie, S Yu, The modeling of graphite oxidation behavior for HTGR fuel coolant channels under normal operating conditions, *Nucl. Eng. Design*, **238** (2008) 2230–2238.
  - 28 M S El-Genk, J-M Tournier, Comparison of oxidation model predictions with gasification data of IG-110, IG-430 and NBG-25 nuclear graphite, *J. Nucl. Mater.*, **420** (2012) 141–158.
  - 29 R C Giberson, J P Walker, Reaction of nuclear graphite with water vapor. Part I: Effect of hydrogen and water vapor partial pressure, *Carbon*, **3** (1966) 521–525.
  - 30 T X Nguyen, J-S Bae, Y Wang, S K Bhatia, On the strength of hydrogen-carbon interactions as deduced from physisorption, *Langmuir*, **25** (2009) 4314–4319.
  - 31 F H Yang, R T Yang, Ab initio molecular orbital study of adsorption of atomic hydrogen on graphite, *Carbon* **40** (2002) 437–444.
  - 32 M B Richards, Reaction of nuclear grade graphite with low concentrations of steam in the helium coolant of an MHTGR, *Energy*, **15** (1990) 729–739.
  - 33 S-H Hsu, S D Stamatidis, J M Carruthers, W N Delgass, V Venkatasubramanian, Bayesian framework for building kinetic models of catalytic systems, *Ind. Eng. Chem. Res.*, **48** (2009) 4768–4790.
  - 34 X Luo, J-C Robin, S Yu, Theoretical analysis of mass transfer and reaction in a porous medium applied to gasification of graphite by water vapor, *Nucl. Eng. Design*, **238** (2008) 2230–2238.
  - 35 M Eto, T Kurosawa, Estimation of graphite materials corrosion with water-vapor in coolant VHTR and oxidation effect on the materials' properties, Specialists meeting on Graphite Component Structural Design, JAERI Tokai (Japan), September 8–11, 1996, IWGGR-11: 189-194.



**ANNEX**



Table A-1: Physical properties of NBG-17 specimens before and after oxidation

Test Data Number	Rejected Tests	Day Number	Test Date	Specimen ID	Before test			Test Conditions			After test			Notes	
					Weight mg	Average L mm	Average D mm	Density g/cm <sup>3</sup>	P H <sub>2</sub> O Pa	P H <sub>2</sub> Pa	Weight mg	Average L mm	Average D mm		Density g/cm <sup>3</sup>
1 - 6		1	12/16/2013	WG1-5	464.92	20.00	3.99	1.859	100	0	459.77	20.00	3.99	1.840	
7 - 13		2	12/17/2013	WG1-6	472.14	20.03	4.01	1.871	50	0	468.67	20.04	4.01	1.855	
14 - 18		3	12/18/2013	WG1-7	452.7	19.86	3.98	1.831	30	0	449.98	19.88	3.98	1.821	
19 - 24		4	1/2/2014	WG1-8	456.55	20.05	3.98	1.832	150	0	450.72	20.05	3.97	1.814	
25 - 30		5	1/6/2014	WG1-9	465.68	20.01	3.99	1.866	300	0	456.19	20.01	3.98	1.831	
31 - 36		6	1/7/2014	WG1-10	467.68	19.99	3.99	1.869	15	0	465.65	19.99	3.99	1.862	
37 - 42		7	1/8/2014	WG1-11	465.53	20.05	3.98	1.867	30	0	463.01	20.05	3.98	1.858	
44 - 48	43	8	1/9/2014	WG1-12	464.35	20.04	3.98	1.860	15	0	462.40	20.04	3.98	1.853	
49 - 54		9	1/13/2014	WG1-13	469.68	19.98	4.00	1.869	50	0	466.11	19.97	4.00	1.859	
55 - 60		10	1/14/2014	WG1-14	472.23	20.04	4.01	1.862	150	0	465.88	20.04	4.01	1.842	
61 - 66		11	1/15/2014	WG1-15	465.1	20.04	3.99	1.856	300	0	456.80	20.04	3.98	1.833	
67 - 72		12	1/16/2014	WG1-16	469.56	19.99	4.01	1.862	100	0	465.96	19.98	4.00	1.856	N1
73 - 78		13	1/21/2014	AG3-1	438.68	20.00	3.99	1.753	50	0	434.80	20.01	3.98	1.748	
79 - 84		14	1/22/2014	AG3-2	462.65	20.06	4.00	1.839	30	0	459.87	20.06	3.98	1.841	
85 - 90		15	1/23/2014	AG3-3	465.83	20.09	3.99	1.851	15	0	464.25	20.09	3.98	1.854	
91 - 96		16	1/24/2014	AG3-4	470.17	20.02	4.00	1.869	100	0	465.59	20.02	4.00	1.852	
97 - 102		17	1/27/2014	AG3-5	454.19	20.01	3.99	1.812	300	0	442.98	20.00	3.98	1.777	
103 - 108		18	1/28/2014	AG3-6	464.52	20.06	4.00	1.844	150	0	458.65	20.06	3.99	1.830	
109 - 114		19	2/5/2014	AG3-7	464.52	20.08	3.99	1.855	300	0	456.02	20.08	3.98	1.825	
115 - 120		20	2/6/2014	AG3-8	463.04	19.91	3.98	1.872	150	0	456.39	19.93	3.97	1.847	
121 - 126		21	2/10/2014	AG3-9	455.72	19.90	3.98	1.840	15	0	452.73	19.91	3.97	1.836	
127 - 132		22	2/11/2014	AG3-10	463.36	19.97	3.98	1.869	30	0	460.81	19.97	3.98	1.855	
133 - 138		23	2/14/2014	AG3-11	464.43	20.02	3.99	1.856	50	0	460.31	20.03	3.98	1.847	
139 - 144		24	2/15/2014	AG3-12	457.97	20.00	3.99	1.836	100	0	452.59	20.00	3.98	1.822	
145 - 150		25	2/16/2014	AG3-13	442.65	20.03	4.00	1.756	0	0	441.12	20.03	4.01	1.748	
151 - 156		26	2/17/2014	AG3-14	465.53	20.05	4.00	1.848	0	0	464.20	20.05	3.99	1.848	
164 - 168	163	28	3/5/2014	AG3-15	463.73	20.09	3.99	1.846	15	30	462.79	20.09	3.99	1.842	N2
172 - 174	169, 170, 171	29	3/6/2014	AG3-16	471.69	19.96	4.02	1.866	30	30	470.47	19.96	4.02	1.859	N2
176 - 180	175	30	3/7/2014	AG3-17	467.5	19.95	3.99	1.871	50	30	465.71	19.95	3.99	1.870	N2
n/a		n/a	3/10/2014	AG3-18	464.33	19.99	3.99	1.860	100	30	463.49	n/a	n/a	n/a	N3
182 - 186	181	31	3/14/2014	AG3-19	460.88	19.97	3.99	1.849	100	30	457.88	19.95	3.99	1.837	N2
189 - 192	187, 188	32	3/25/2014	AG3-20	453.58	20.09	3.98	1.814	150	30	448.41	20.09	3.98	1.797	N2
n/a		n/a	3/27/2014	AG3-21	467.18	19.99	4.02	1.842	300	30	457.54	19.99	4.02	1.808	
n/a		n/a	3/31/2014	AG3-22	456.19	19.83	3.98	1.846	15	0	454.09	19.83	3.98	1.844	N1
195 - 198	193, 194	33	4/1/2014	WG1-17	468.16	19.98	4.00	1.862	100	30	464.68	19.99	4.00	1.850	
201 - 204	199, 200	34	4/2/2014	WG1-18	468.16	20.01	3.99	1.868	50	30	462.35	20.01	3.99	1.847	
208, 210	205, 206, 207, 209	35	4/3/2014	WG1-19	464.23	20.04	3.99	1.856	30	30	462.70	20.04	3.98	1.852	N2

Test Data Number	Rejected Tests	Day Number	Test Date	Specimen ID	Before test			Test Conditions			After test			Notes	
					Weight mg	Average L mm	Average D mm	Density g/cm <sup>3</sup>	P H <sub>2</sub> O Pa	P H <sub>2</sub> Pa	Weight mg	Average L mm	Average D mm		Density g/cm <sup>3</sup>
213 - 216	211, 212	36	4/4/2014	WG1-20	465.3	20.03	3.98	1.865	150	30	460.74	20.04	3.98	1.846	
217 - 222	219	37	4/7/2014	WG1-21	466.16	20.03	3.99	1.861	300	30	459.19	20.01	3.99	1.839	
225 - 227	223, 224	38	4/8/2014	WG1-22	457.51	19.80	3.99	1.844	15	30	456.71	19.81	3.99	1.845	N1
	228 - 233	39	4/9/2014	WG1-23	470.38	20.01	4.00	1.871	3	100	469.74	20.02	4.01	1.863	N5
234 - 239	239	40	6/30/2014	WG1-24	465.29	20.07	3.99	1.853	500	0	442.02	20.07	3.98	1.774	
240 - 244	245, 246	41	7/1/2014	WG1-25	465.38	20.05	3.98	1.868	1000	0	430.71	20.04	3.96	1.742	N1
			7/3/2014	WG1-26	468.94	20.00	4.00	1.866	750	0	467.95	19.99	4.00	1.861	N4
247 - 251		42	7/29/2014	WG1-27	467.87	20.02	3.99	1.865	100	30	465.72	20.01	3.99	1.861	N6
252 - 255		43	8/4/2014	WG1-28	466.22	20.01	3.99	1.863	100	30	464.77	20.02	3.98	1.864	N6
256 - 263		44	8/8/2014	WG1-29	466.01	20.03	3.98	1.868	100-200	vary	464.60	20.04	3.99	1.853	
264 - 272		45	8/12/2014	WG1-30	466.83	20.04	4.00	1.859	30-50	vary	465.87	20.03	3.99	1.860	
272 - 282	273, 274, 276	46	8/15/2014	WG1-31	470.25	19.99	4.01	1.868	vary	25	469.58	19.99	4.01	1.861	
283 - 286		47	8/25/2014	WG1-32	456.9	20.02	4.00	1.818	15	26	456.34	20.03	4.00	1.816	
287 - 290		48	9/3/2014	WG1-33	463.92	20.06	3.98	1.857	30	26	463.15	20.05	3.98	1.861	
291 - 294		49	12/30/2014	WG1-34-1	468.3	20.01	3.99	1.869	30	0	n/a	n/a	n/a	n/a	N5
291 - 296		50	1/1/2015	WG1-34-2	n/a	n/a	n/a	n/a	15	0	n/a	n/a	n/a	n/a	N5
297 - 300		51	1/5/2015	WG1-34-3	n/a	n/a	n/a	n/a	3	0	n/a	n/a	n/a	n/a	
301 - 304		52	1/7/2015	WG1-34-4	n/a	n/a	n/a	n/a	3	0	464.80	20.02	4.00	1.850	

Notes:

- N1 Poor control on P<sub>K2O</sub>
- N2 Errors in slow oxidaiton rates
- N3 Helium flow stopped during test
- N4 Hygrometer malfunction
- N5 Fluctuations in helium flow
- N5 No H<sub>2</sub>O, 100 Pa H<sub>2</sub> in He
- N6 H<sub>2</sub> on at off at 850 oC

Table A-2: Experimental oxidation rates and corresponding conditions

Test Data Number	Day Number	Test Date	Specimen ID	Water Pressure		H2 Pressure	Temperature		Weight		Time in the Test		Oxidation Rate	Burn off %		Sample Preparation		Weight Loss on Outgasing	Notes
				target	actual		target	actual	before	after	before	after		before	after	duration	temperature		
				Pa	Pa	Pa	°C	°C	mg	mg	hr	hr	s <sup>-1</sup>	%	%	h	°C	mg	
1	1	12/16/2013	WG1-5	100	100	0	800	800	465.07	465.04	4.60	7.36	5.84E-09	-0.03	-0.03	1	1200	0.18	
2	1	12/16/2013	WG1-5	100	101	0	850	850	464.99	464.91	7.70	10.46	1.71E-08	-0.01	0.00	1	1200	0.18	
3	1	12/16/2013	WG1-5	100	101	0	900	900	464.84	464.72	10.91	13.56	2.73E-08	0.02	0.04	1	1200	0.18	
4	1	12/16/2013	WG1-5	100	101	0	950	950	464.66	464.41	13.78	16.55	5.42E-08	0.06	0.11	1	1200	0.18	
5	1	12/16/2013	WG1-5	100	101	0	1000	1000	464.30	463.68	16.94	19.68	1.35E-07	0.13	0.27	1	1200	0.18	
6	1	12/16/2013	WG1-5	100	100	0	1100	1100	463.29	460.17	20.12	22.86	6.81E-07	0.35	1.02	1	1200	0.18	
7	2	12/17/2013	WG1-6	50	50	0	800	800	471.18	471.14	4.21	7.34	7.53E-09	0.17	0.18	1	1200	0.15	
8	2	12/17/2013	WG1-6	50	51	0	850	850	471.07	471.02	7.81	10.46	1.27E-08	0.19	0.21	1	1200	0.15	
9	2	12/17/2013	WG1-6	50	50	0	900	900	470.96	470.85	10.82	13.51	2.46E-08	0.22	0.24	1	1200	0.15	
10	2	12/17/2013	WG1-6	50	51	0	950	950	470.74	470.57	13.90	16.57	3.71E-08	0.27	0.30	1	1200	0.15	
11	2	12/17/2013	WG1-6	50	51	0	1000	1000	470.46	470.05	17.02	19.68	9.21E-08	0.32	0.41	1	1200	0.15	
12	2	12/17/2013	WG1-6	50	51	0	1100	1100	469.75	467.86	20.15	22.86	4.11E-07	0.47	0.87	1	1200	0.15	
13	3	12/18/2013	WG1-7	30	30	0	800	800	451.65	451.63	4.52	6.61	6.18E-09	0.20	0.20	2	1200	0.15	
14	3	12/18/2013	WG1-7	30	30	0	850	850	451.54	451.47	7.89	10.43	1.77E-08	0.22	0.24	2	1200	0.15	
15	3	12/18/2013	WG1-7	30	30	0	900	900	451.40	451.31	10.94	13.48	2.30E-08	0.25	0.27	2	1200	0.15	
16	3	12/18/2013	WG1-7	30	30	0	950	950	451.24	451.08	13.95	16.57	3.69E-08	0.29	0.32	2	1200	0.15	
17	3	12/18/2013	WG1-7	30	30	0	1000	1000	450.99	450.67	17.02	19.70	7.33E-08	0.34	0.42	2	1200	0.15	
18	3	12/18/2013	WG1-7	30	30	0	1100	1100	450.48	449.25	20.04	22.66	2.90E-07	0.46	0.73	2	1200	0.15	
19	4	1/2/2014	WG1-8	150	152	0	800	800	455.29	455.26	4.85	7.39	7.45E-09	0.23	0.23	2	1200	0.22	
20	4	1/2/2014	WG1-8	150	153	0	850	850	455.21	455.15	7.84	10.38	1.44E-08	0.25	0.26	2	1200	0.22	
21	4	1/2/2014	WG1-8	150	153	0	900	900	455.08	454.97	10.85	13.51	2.59E-08	0.27	0.30	2	1200	0.22	
22	4	1/2/2014	WG1-8	150	152	0	950	950	454.90	454.67	13.93	16.57	5.25E-08	0.31	0.36	2	1200	0.22	
23	4	1/2/2014	WG1-8	150	151	0	1000	1000	454.57	453.93	16.94	19.73	1.40E-07	0.39	0.53	2	1200	0.22	
24	4	1/2/2014	WG1-8	150	150	0	1100	1100	453.47	449.73	20.18	22.94	8.30E-07	0.63	1.45	2	1200	0.22	
25	5	1/6/2014	WG1-9	300	303	0	800	800	464.463	464.427	4.46	7.24	7.74E-09	0.21	0.22	2	1200	0.22	
26	5	1/6/2014	WG1-9	300	302	0	850	850	464.367	464.31	7.80	10.38	1.32E-08	0.24	0.25	2	1200	0.22	
27	5	1/6/2014	WG1-9	300	304	0	900	900	464.248	464.125	10.80	13.47	2.76E-08	0.26	0.29	2	1200	0.22	
28	5	1/6/2014	WG1-9	300	307	0	950	950	464.045	463.729	13.69	16.64	6.41E-08	0.30	0.37	2	1200	0.22	
29	5	1/6/2014	WG1-9	300	309	0	1000	1000	463.582	462.677	17.03	19.70	2.03E-07	0.40	0.60	2	1200	0.22	
30	5	1/6/2014	WG1-9	300	314	0	1100	1100	462.139	455.456	20.09	22.92	1.42E-06	0.71	2.15	2	1200	0.22	
31	6	1/7/2014	WG1-10	15	15	0	800	800	466.664	466.628	4.71	7.28	8.34E-09	0.18	0.19	2	1200	0.16	
32	6	1/7/2014	WG1-10	15	15	0	850	850	466.571	466.5	7.81	10.41	1.63E-08	0.20	0.22	2	1200	0.16	
33	6	1/7/2014	WG1-10	15	15	0	900	900	466.44	466.348	10.85	13.51	2.06E-08	0.23	0.25	2	1200	0.16	
34	6	1/7/2014	WG1-10	15	15	0	950	950	466.279	466.141	13.95	16.63	3.07E-08	0.27	0.29	2	1200	0.16	
35	6	1/7/2014	WG1-10	15	15	0	1000	1000	466.07	465.81	16.91	19.70	5.55E-08	0.31	0.37	2	1200	0.16	
36	6	1/7/2014	WG1-10	15	15	0	1100	1100	465.629	464.813	20.07	22.86	1.74E-07	0.40	0.58	2	1200	0.16	
37	7	1/8/2014	WG1-11	30	30	0	800	800	464.557	464.518	4.63	7.45	8.27E-09	0.18	0.19	2	1200	0.14	
38	7	1/8/2014	WG1-11	30	30	0	850	850	464.465	464.398	7.73	10.49	1.45E-08	0.20	0.21	2	1200	0.14	
39	7	1/8/2014	WG1-11	30	32	0	900	900	464.339	464.234	10.80	13.64	2.21E-08	0.23	0.25	2	1200	0.14	
40	7	1/8/2014	WG1-11	30	32	0	950	950	464.176	464.012	13.81	16.66	3.44E-08	0.26	0.30	2	1200	0.14	
41	7	1/8/2014	WG1-11	30	32	0	1000	1000	463.939	463.613	16.88	19.73	6.85E-08	0.31	0.38	2	1200	0.14	
42	7	1/8/2014	WG1-11	30	32	0	1100	1100	463.406	462.082	20.07	22.91	2.79E-07	0.43	0.71	2	1200	0.14	
44	8	1/9/2014	WG1-12	15	15	0	850	850	463.261	463.181	7.87	10.46	1.85E-08	0.20	0.22	2	1200	0.14	
45	8	1/9/2014	WG1-12	15	15	0	900	900	463.123	463.021	10.77	13.62	2.15E-08	0.23	0.26	2	1200	0.14	
46	8	1/9/2014	WG1-12	15	15	0	950	950	462.956	462.812	13.90	16.52	3.30E-08	0.27	0.30	2	1200	0.14	
47	8	1/9/2014	WG1-12	15	15	0	1000	1000	462.727	462.455	16.94	19.70	5.92E-08	0.32	0.38	2	1200	0.14	
48	8	1/9/2014	WG1-12	15	16	0	1100	1100	462.185	461.413	20.34	22.89	1.82E-07	0.44	0.60	2	1200	0.14	
49	9	1/13/2014	WG1-13	50	49	0	800	800	468.56	468.515	4.54	7.47	9.10E-09	0.20	0.21	2	1200	0.16	
50	9	1/13/2014	WG1-13	50	49	0	850	850	468.461	468.393	7.67	10.46	1.45E-08	0.22	0.24	2	1200	0.16	
51	9	1/13/2014	WG1-13	50	49	0	900	900	468.334	468.224	10.74	13.56	2.31E-08	0.25	0.28	2	1200	0.16	
52	9	1/13/2014	WG1-13	50	49	0	950	950	468.158	467.956	13.81	16.66	4.21E-08	0.29	0.33	2	1200	0.16	
53	9	1/13/2014	WG1-13	50	49	0	1000	1000	467.881	467.458	16.86	19.76	8.66E-08	0.35	0.44	2	1200	0.16	

Test Data Number	Day Number	Test Date	Specimen ID	Water Pressure		H2 Pressure	Temperature		Weight		Time in the Test		Oxidation Rate	Burn off %		Sample Preparation		Weight Loss on Outgasing	Notes
				target	actual		target	actual	before	after	before	after		before	after	duration	temperature		
				Pa	Pa	Pa	°C	°C	mg	mg	hr	hr	s <sup>-1</sup>	%	%	h	°C	mg	
54	9	1/13/2014	WG1-13	50	49	0	1100	1100	467.205	465.372	20.09	22.89	3.89E-07	0.49	0.88	2	1200	0.16	
55	10	1/14/2014	WG1-14	150	149	0	800	800	471.241	471.21	4.82	7.39	7.11E-09	0.18	0.19	2	1200	0.15	
56	10	1/14/2014	WG1-14	150	150	0	850	850	471.156	471.062	7.67	10.43	2.01E-08	0.20	0.22	2	1200	0.15	
57	10	1/14/2014	WG1-14	150	152	0	900	900	470.999	470.845	10.74	13.56	3.22E-08	0.23	0.26	2	1200	0.15	
58	10	1/14/2014	WG1-14	150	155	0	950	950	470.771	470.485	13.84	16.60	6.11E-08	0.28	0.34	2	1200	0.15	
59	10	1/14/2014	WG1-14	150	158	0	1000	1000	470.358	469.646	16.99	19.73	1.53E-07	0.37	0.52	2	1200	0.15	
60	10	1/14/2014	WG1-14	150	160	0	1100	1100	469.237	465.093	20.09	22.86	8.86E-07	0.60	1.48	2	1200	0.15	
61	11	1/15/2014	WG1-15	300	304	0	800	800	464.077	464.053	4.36	7.28	4.92E-09	0.19	0.19	2	1200	0.15	
62	11	1/15/2014	WG1-15	300	306	0	850	850	463.994	463.914	7.75	10.45	1.77E-08	0.21	0.22	2	1200	0.15	
63	11	1/15/2014	WG1-15	300	306	0	900	900	463.846	463.726	10.89	13.51	2.74E-08	0.24	0.26	2	1200	0.15	
64	11	1/15/2014	WG1-15	300	310	0	950	950	463.648	463.337	13.84	16.60	6.75E-08	0.28	0.35	2	1200	0.15	
65	11	1/15/2014	WG1-15	300	316	0	1000	1000	463.207	462.319	16.96	19.77	1.90E-07	0.37	0.57	2	1200	0.15	
66	11	1/15/2014	WG1-15	300	327	0	1100	1100	461.341	456.033	20.37	22.88	1.27E-06	0.78	1.92	2	1200	0.15	
67	12	1/16/2014	WG1-16	100	101	0	800	800	468.502	468.471	4.60	7.34	6.71E-09	0.19	0.20	2	1200	0.16	
68	12	1/16/2014	WG1-16	100	101	0	850	850	468.417	468.344	7.61	10.49	1.50E-08	0.21	0.22	2	1200	0.16	
69	12	1/16/2014	WG1-16	100	61	0	900	900	468.286	468.177	10.74	13.56	2.29E-08	0.24	0.26	2	1200	0.16	
70	12	1/16/2014	WG1-16	100	60	0	950	950	468.109	467.901	13.81	16.63	4.38E-08	0.28	0.32	2	1200	0.16	
71	12	1/16/2014	WG1-16	100	60	0	1000	1000	467.825	467.375	16.86	19.73	9.31E-08	0.34	0.43	2	1200	0.16	
72	12	1/16/2014	WG1-16	100	60	0	1100	1100	467.09	465.026	20.12	22.91	4.40E-07	0.49	0.93	2	1200	0.16	
73	13	1/21/2014	AG3-1	50	51	0	800	800	437.532	437.501	4.82	7.39	7.66E-09	0.22	0.23	2	1200	0.19	
74	13	1/21/2014	AG3-1	50	51	0	850	850	437.447	437.384	7.73	10.52	1.43E-08	0.24	0.25	2	1200	0.19	
75	13	1/21/2014	AG3-1	50	51	0	900	900	437.327	437.226	10.77	13.56	2.30E-08	0.27	0.29	2	1200	0.19	
76	13	1/21/2014	AG3-1	50	51	0	950	950	437.166	436.967	13.76	16.63	4.41E-08	0.30	0.35	2	1200	0.19	
77	13	1/21/2014	AG3-1	50	51	0	1000	1000	436.877	436.445	16.94	19.70	9.95E-08	0.37	0.47	2	1200	0.19	
78	13	1/21/2014	AG3-1	50	50	0	1100	1100	436.103	434.047	20.21	22.91	4.85E-07	0.54	1.01	2	1200	0.19	
79	14	1/22/2014	AG3-2	30	31	0	800	800	461.685	461.629	4.79	7.47	1.26E-08	0.18	0.19	2	1200	0.13	
80	14	1/22/2014	AG3-2	30	32	0	850	850	461.578	461.513	7.70	10.52	1.39E-08	0.20	0.22	2	1200	0.13	
81	14	1/22/2014	AG3-2	30	32	0	900	900	461.436	461.355	10.80	13.56	1.77E-08	0.23	0.25	2	1200	0.13	
82	14	1/22/2014	AG3-2	30	31	0	950	950	461.296	461.113	13.76	16.69	3.76E-08	0.26	0.30	2	1200	0.13	
83	14	1/22/2014	AG3-2	30	32	0	1000	1000	461.038	460.649	16.91	19.76	8.22E-08	0.32	0.40	2	1200	0.13	
84	14	1/22/2014	AG3-2	30	32	0	1100	1100	460.432	458.989	20.07	22.91	3.07E-07	0.45	0.76	2	1200	0.13	
85	15	1/23/2014	AG3-3	15	16	0	800	800	464.874	464.831	4.61	7.34	9.41E-09	0.18	0.19	2	1200	0.13	
86	15	1/23/2014	AG3-3	15	16	0	850	850	464.774	464.714	7.71	10.56	1.26E-08	0.20	0.21	2	1200	0.13	
87	15	1/23/2014	AG3-3	15	16	0	900	900	464.659	464.573	10.77	13.59	1.82E-08	0.22	0.24	2	1200	0.13	
88	15	1/23/2014	AG3-3	15	16	0	950	950	464.511	464.381	13.86	16.68	2.76E-08	0.26	0.28	2	1200	0.13	
89	15	1/23/2014	AG3-3	15	16	0	1000	1000	464.311	464.053	16.91	19.70	5.53E-08	0.30	0.35	2	1200	0.13	
90	15	1/23/2014	AG3-3	15	16	0	1100	1100	463.865	463.312	20.10	22.16	1.61E-07	0.39	0.51	2	1200	0.13	
91	16	1/24/2014	AG3-4	100	102	0	800	800	469.193	469.17	5.49	7.39	7.17E-09	0.18	0.19	2	1200	0.12	
92	16	1/24/2014	AG3-4	100	102	0	850	850	469.117	469.058	7.76	10.52	1.27E-08	0.20	0.21	2	1200	0.12	
93	16	1/24/2014	AG3-4	100	102	0	900	900	468.994	468.883	10.91	13.56	2.48E-08	0.23	0.25	2	1200	0.12	
94	16	1/24/2014	AG3-4	100	102	0	950	950	468.812	468.577	13.87	16.69	4.94E-08	0.26	0.31	2	1200	0.12	
95	16	1/24/2014	AG3-4	100	102	0	1000	1000	468.489	467.919	16.91	19.76	1.19E-07	0.33	0.45	2	1200	0.12	
96	16	1/24/2014	AG3-4	100	101	0	1100	1100	467.573	464.765	20.12	22.89	6.02E-07	0.53	1.12	2	1200	0.12	
97	17	1/27/2014	AG3-5	300	299	0	800	800	453.06	453.005	4.77	7.38	1.29E-08	0.20	0.22	2	1200	0.20	
98	17	1/27/2014	AG3-5	300	302	0	850	850	452.941	452.858	7.86	10.44	1.97E-08	0.23	0.25	2	1200	0.20	
99	17	1/27/2014	AG3-5	300	303	0	900	900	452.797	452.651	10.74	13.55	3.19E-08	0.26	0.29	2	1200	0.20	
100	17	1/27/2014	AG3-5	300	306	0	950	950	452.579	452.211	13.80	16.67	7.87E-08	0.31	0.39	2	1200	0.20	
101	17	1/27/2014	AG3-5	300	308	0	1000	1000	452.083	450.983	16.94	19.78	2.38E-07	0.42	0.66	2	1200	0.20	
102	17	1/27/2014	AG3-5	300	310	0	1100	1100	450.657	442.425	19.98	22.86	1.76E-06	0.73	2.55	2	1200	0.20	
103	18	1/28/2014	AG3-6	150	150	0	800	800	463.513	463.468	4.63	7.39	9.77E-09	0.19	0.20	2	1200	0.15	
104	18	1/28/2014	AG3-6	150	150	0	850	850	463.416	463.346	7.61	10.46	1.47E-08	0.21	0.22	2	1200	0.15	
105	18	1/28/2014	AG3-6	150	151	0	900	900	463.289	463.175	10.74	13.51	2.47E-08	0.23	0.26	2	1200	0.15	
106	18	1/28/2014	AG3-6	150	151	0	950	950	463.107	462.841	13.78	16.66	5.54E-08	0.27	0.33	2	1200	0.15	

Test Data Number	Day Number	Test Date	Specimen ID	Water Pressure		H2 Pressure	Temperature		Weight		Time in the Test		Oxidation Rate	Burn off %		Sample Preparation		Weight Loss on Outgasing	Notes
				target	actual		target	actual	before	after	before	after		before	after	duration	temperature		
				Pa	Pa	Pa	°C	°C	mg	mg	hr	hr	s <sup>-1</sup>	%	%	h	°C	mg	
107	18	1/28/2014	AG3-6	150	151	0	1000	1000	462.763	462.042	16.83	19.81	1.45E-07	0.35	0.50	2	1200	0.15	
108	18	1/28/2014	AG3-6	150	151	0	1100	1100	461.647	457.782	20.12	22.91	8.34E-07	0.59	1.42	2	1200	0.15	
109	19	2/5/2014	AG3-7	300	305	0	800	800	463.67	463.623	4.33	7.34	9.35E-09	0.20	0.21	2	1200	0.16	
110	19	2/5/2014	AG3-7	300	306	0	850	850	463.565	463.484	7.67	10.43	1.76E-08	0.22	0.24	2	1200	0.16	
111	19	2/5/2014	AG3-7	300	306	0	900	900	463.42	463.286	10.81	13.54	2.94E-08	0.25	0.28	2	1200	0.16	
112	19	2/5/2014	AG3-7	300	306	0	950	950	463.206	462.891	13.87	16.63	6.84E-08	0.30	0.36	2	1200	0.16	
113	19	2/5/2014	AG3-7	300	305	0	1000	1000	462.783	461.878	16.90	19.79	1.88E-07	0.39	0.58	2	1200	0.16	
114	19	2/5/2014	AG3-7	300	307	0	1100	1100	461.696	455.617	19.93	22.77	1.29E-06	0.62	1.93	2	1200	0.16	
115	20	2/6/2014	AG3-8	150	150	0	800	800	461.912	461.838	4.88	7.34	1.81E-08	0.20	0.22	2	1200	0.20	
116	20	2/6/2014	AG3-8	150	152	0	850	850	461.778	461.666	7.70	10.46	2.44E-08	0.23	0.25	2	1200	0.20	
117	20	2/6/2014	AG3-8	150	151	0	900	900	461.601	461.432	10.77	13.56	3.65E-08	0.27	0.30	2	1200	0.20	
118	20	2/6/2014	AG3-8	150	152	0	950	950	461.353	461.04	13.87	16.60	6.90E-08	0.32	0.39	2	1200	0.20	
119	20	2/6/2014	AG3-8	150	151	0	1000	1000	460.937	460.182	16.88	19.68	1.62E-07	0.41	0.57	2	1200	0.20	
120	20	2/6/2014	AG3-8	150	152	0	1100	1100	459.642	455.378	20.18	22.91	9.44E-07	0.69	1.61	2	1200	0.20	
121	21	2/10/2014	AG3-9	15	15	0	800	800	460.261	460.211	5.35	7.34	1.52E-08	0.25	0.26	2	1200	0.32	
122	21	2/10/2014	AG3-9	15	15	0	850	850	460.149	460.049	7.70	10.52	2.14E-08	0.27	0.29	2	1200	0.32	
123	21	2/10/2014	AG3-9	15	15	0	900	900	459.986	459.846	10.80	13.53	3.10E-08	0.31	0.34	2	1200	0.32	
124	21	2/10/2014	AG3-9	15	15	0	950	950	459.777	459.533	13.78	16.74	4.98E-08	0.35	0.40	2	1200	0.32	
125	21	2/10/2014	AG3-9	15	15	0	1000	1000	459.462	459.092	16.97	19.73	8.10E-08	0.42	0.50	2	1200	0.32	
126	21	2/10/2014	AG3-9	15	15	0	1100	1100	458.882	457.906	20.09	22.89	2.11E-07	0.55	0.76	2	1200	0.32	
127	22	2/11/2014	AG3-10	30	31	0	800	800	462.401	462.351	4.52	7.31	1.08E-08	0.18	0.19	2	1200	0.14	
128	22	2/11/2014	AG3-10	30	31	0	850	850	462.288	462.166	7.76	10.49	2.69E-08	0.20	0.23	2	1200	0.14	
129	22	2/11/2014	AG3-10	30	31	0	900	900	462.106	461.963	10.77	13.56	3.08E-08	0.24	0.27	2	1200	0.14	
130	22	2/11/2014	AG3-10	30	31	0	950	950	461.896	461.687	13.81	16.69	4.36E-08	0.29	0.33	2	1200	0.14	
131	22	2/11/2014	AG3-10	30	31	0	1000	1000	461.613	461.259	16.88	19.76	7.40E-08	0.35	0.42	2	1200	0.14	
132	22	2/11/2014	AG3-10	30	31	0	1100	1100	461.047	459.807	20.09	22.94	2.62E-07	0.47	0.74	2	1200	0.14	
133	23	2/14/2014	AG3-11	50	51	0	800	800	463.228	463.159	4.77	7.42	1.56E-08	0.22	0.23	2	1200	0.20	
134	23	2/14/2014	AG3-11	50	51	0	850	850	463.099	463.003	7.76	10.41	2.17E-08	0.24	0.26	2	1200	0.20	
135	23	2/14/2014	AG3-11	50	51	0	900	900	462.932	462.8	10.88	13.51	3.01E-08	0.28	0.31	2	1200	0.20	
136	23	2/14/2014	AG3-11	50	50	0	950	950	462.723	462.472	13.84	16.60	5.46E-08	0.33	0.38	2	1200	0.20	
137	23	2/14/2014	AG3-11	50	48	0	1000	1000	462.379	461.866	16.88	19.68	1.10E-07	0.40	0.51	2	1200	0.20	
138	23	2/14/2014	AG3-11	50	50	0	1100	1100	461.565	459.353	20.09	22.91	4.72E-07	0.57	1.05	2	1200	0.20	
139	24	2/15/2014	AG3-12	100	105	0	800	800	456.892	456.821	4.24	7.39	1.37E-08	0.19	0.21	2	1200	0.20	
140	24	2/15/2014	AG3-12	100	102	0	850	850	456.767	456.665	7.64	10.49	2.18E-08	0.22	0.24	2	1200	0.20	
141	24	2/15/2014	AG3-12	100	102	0	900	900	456.603	456.445	10.74	13.62	3.34E-08	0.26	0.29	2	1200	0.20	
142	24	2/15/2014	AG3-12	100	102	0	950	950	456.373	456.093	13.84	16.69	5.98E-08	0.31	0.37	2	1200	0.20	
143	24	2/15/2014	AG3-12	100	102	0	1000	1000	455.999	455.387	16.91	19.68	1.35E-07	0.39	0.52	2	1200	0.20	
144	24	2/15/2014	AG3-12	100	101	0	1100	1100	454.91	451.662	20.21	22.94	7.26E-07	0.63	1.34	2	1200	0.20	
145	25	2/16/2014	AG3-13	3	3	0	800	800	441.532	441.472	4.04	7.39	1.13E-08	0.22	0.23	2	1200	0.15	
146	25	2/16/2014	AG3-13	3	3	0	850	850	441.414	441.273	7.61	10.49	3.08E-08	0.25	0.28	2	1200	0.15	
147	25	2/16/2014	AG3-13	3	3	0	900	900	441.207	441.06	10.74	13.56	3.28E-08	0.29	0.33	2	1200	0.15	
148	25	2/16/2014	AG3-13	3	3	0	950	950	440.988	440.848	13.87	16.63	3.20E-08	0.34	0.37	2	1200	0.15	
149	25	2/16/2014	AG3-13	3	3	0	1000	1000	440.774	440.6	16.94	19.76	3.89E-08	0.39	0.43	2	1200	0.15	
150	25	2/16/2014	AG3-13	3	3	0	1100	1100	440.452	440.148	20.07	22.94	6.68E-08	0.46	0.53	2	1200	0.15	
151	26	2/17/2014	AG3-14	3	3	0	800	800	464.54	464.468	4.07	7.36	1.31E-08	0.18	0.20	2	1200	0.15	
152	26	2/17/2014	AG3-14	3	3	0	850	850	464.406	464.291	7.70	10.52	2.44E-08	0.21	0.24	2	1200	0.15	
153	26	2/17/2014	AG3-14	3	3	0	900	900	464.24	464.096	10.71	13.64	2.94E-08	0.25	0.28	2	1200	0.15	
154	26	2/17/2014	AG3-14	3	3	0	950	950	464.033	463.873	13.81	16.57	3.47E-08	0.29	0.32	2	1200	0.15	
155	26	2/17/2014	AG3-14	3	3	0	1000	1000	463.795	463.636	16.91	19.65	3.48E-08	0.34	0.38	2	1200	0.15	
156	26	2/17/2014	AG3-14	3	3	0	1100	1100	463.477	463.178	20.07	22.89	6.35E-08	0.41	0.47	2	1200	0.15	
157	27	3/31/2014	AG3-22	15	24	0	800	800	454.981	454.911	4.68	7.42	1.56E-08	0.22	0.23	2	1200	0.21	
158	27	3/31/2014	AG3-22	15	23	0	850	850	454.85	454.772	7.73	10.49	1.73E-08	0.25	0.27	2	1200	0.21	
159	27	3/31/2014	AG3-22	15	22	0	900	900	454.707	454.595	10.88	13.62	2.50E-08	0.28	0.30	2	1200	0.21	

Test Data Number	Day Number	Test Date	Specimen ID	Water Pressure		H2 Pressure	Temperature		Weight		Time in the Test		Oxidation Rate	Burn off %		Sample Preparation		Weight Loss on Outgasing	Notes
				target	actual		target	actual	before	after	before	after		before	after	duration	temperature		
				Pa	Pa	Pa	°C	°C	mg	mg	hr	hr	s <sup>-1</sup>	%	%	h	°C	mg	
160	27	3/31/2014	AG3-22	15	21	0	950	950	454.524	454.33	13.87	16.63	4.30E-08	0.32	0.36	2	1200	0.21	
161	27	3/31/2014	AG3-22	15	22	0	1000	1000	454.249	453.891	16.88	19.76	7.60E-08	0.38	0.46	2	1200	0.21	
162	27	3/31/2014	AG3-22	15	8	0	1100	1100	453.658	453.042	20.12	22.91	1.35E-07	0.51	0.64	2	1200	0.21	
164	28	3/5/2014	AG3-15	30	15	26	850	850	462.701	462.703	7.78	10.43	-4.53E-10	0.19	0.19	2	1200	0.16	
165	28	3/5/2014	AG3-15	30	15	26	900	900	462.652	462.639	10.85	13.56	2.88E-09	0.20	0.20	2	1200	0.16	
166	28	3/5/2014	AG3-15	30	15	26	950	950	462.584	462.555	13.87	16.60	6.38E-09	0.21	0.22	2	1200	0.16	
167	28	3/5/2014	AG3-15	30	15	26	1000	1000	462.494	462.419	16.97	19.68	1.66E-08	0.23	0.25	2	1200	0.16	
168	28	3/5/2014	AG3-15	30	15	26	1100	1100	462.271	461.95	20.12	22.83	7.12E-08	0.28	0.35	2	1200	0.16	
172	29	3/6/2014	AG3-16	30	29	26	950	950	470.614	470.576	13.98	16.63	8.46E-09	0.20	0.21	2	1200	0.12	
173	29	3/6/2014	AG3-16	30	29	26	1000	1000	470.51	470.406	16.99	19.76	2.22E-08	0.22	0.25	2	1200	0.12	
174	29	3/6/2014	AG3-16	30	29	26	1100	1100	470.222	469.564	20.07	22.94	1.35E-07	0.29	0.42	2	1200	0.12	
176	30	3/7/2014	AG3-17	50	52	26	850	850	466.444	466.438	7.70	10.55	1.25E-09	0.19	0.19	2	1200	0.15	
177	30	3/7/2014	AG3-17	50	51	26	900	900	466.385	466.35	10.77	13.51	7.61E-09	0.21	0.21	2	1200	0.15	
178	30	3/7/2014	AG3-17	50	51	26	950	950	466.29	466.215	13.84	16.69	1.57E-08	0.23	0.24	2	1200	0.15	
179	30	3/7/2014	AG3-17	50	51	26	1000	1000	466.148	465.958	16.91	19.76	3.97E-08	0.26	0.30	2	1200	0.15	
180	30	3/7/2014	AG3-17	50	51	26	1100	1100	465.767	464.757	20.09	22.84	2.19E-07	0.34	0.55	2	1200	0.15	
182	31	3/14/2014	AG3-19	100	100	26	850	850	459.711	459.703	7.87	10.52	1.82E-09	0.21	0.21	2	1200	0.22	
183	31	3/14/2014	AG3-19	100	100	26	900	900	459.652	459.639	10.77	13.51	2.87E-09	0.22	0.22	2	1200	0.22	
184	31	3/14/2014	AG3-19	100	99	26	950	950	459.575	459.478	13.95	16.66	2.16E-08	0.24	0.26	2	1200	0.22	
185	31	3/14/2014	AG3-19	100	99	26	1000	1000	459.401	459.086	16.94	19.73	6.83E-08	0.27	0.34	2	1200	0.22	
186	31	3/14/2014	AG3-19	100	98	26	1100	1100	458.788	458.109	20.18	21.24	3.88E-07	0.41	0.55	2	1200	0.22	
189	32	3/25/2014	AG3-20	150	152	26	900	900	452.222	452.195	10.74	13.51	5.99E-09	0.25	0.26	2	1200	0.22	
190	32	3/25/2014	AG3-20	150	151	26	950	950	452.137	451.999	13.78	16.69	2.91E-08	0.27	0.30	2	1200	0.22	
191	32	3/25/2014	AG3-20	150	151	26	1000	1000	451.926	451.421	16.86	19.79	1.06E-07	0.32	0.43	2	1200	0.22	
192	32	3/25/2014	AG3-20	150	151	26	1100	1100	451.018	447.52	20.15	23.00	7.56E-07	0.52	1.29	2	1200	0.22	
195	33	4/1/2014	WG1-17	100	103	26	900	900	466.935	466.924	10.80	13.58	2.35E-09	0.22	0.22	2	1200	0.17	
196	33	4/1/2014	WG1-17	100	102	26	950	950	466.865	466.77	13.78	16.63	1.98E-08	0.23	0.25	2	1200	0.17	
197	33	4/1/2014	WG1-17	100	103	26	1000	1000	466.697	466.318	16.88	19.73	7.92E-08	0.27	0.35	2	1200	0.17	
198	33	4/1/2014	WG1-17	100	103	26	1100	1100	466.064	463.773	20.07	22.97	4.71E-07	0.41	0.90	2	1200	0.17	
201	34	4/2/2014	WG1-18	50	51	26	900	900	463.309	463.301	10.71	13.59	1.67E-09	0.22	0.22	2	1200	0.18	
202	34	4/2/2014	WG1-18	50	52	26	950	950	463.244	463.173	13.84	16.69	1.49E-08	0.23	0.25	2	1200	0.18	
203	34	4/2/2014	WG1-18	50	52	26	1000	1000	463.103	462.838	16.91	19.79	5.52E-08	0.27	0.32	2	1200	0.18	
204	34	4/2/2014	WG1-18	50	52	26	1100	1100	462.635	461.385	20.07	22.91	2.64E-07	0.37	0.64	2	1200	0.18	
208	35	4/3/2014	WG1-19	30	30	26	950	950	463.009	462.969	13.82	16.64	8.51E-09	0.23	0.24	2	1200	0.17	
210	35	4/3/2014	WG1-19	30	30	26	1100	1100	462.525	461.739	20.10	22.89	1.69E-07	0.33	0.50	2	1200	0.17	
213	36	4/4/2014	WG1-20	150	150	26	900	900	464.163	464.149	10.85	13.56	3.09E-09	0.21	0.21	2	1200	0.15	
214	36	4/4/2014	WG1-20	150	150	26	950	950	464.086	463.955	13.87	16.63	2.84E-08	0.23	0.26	2	1200	0.15	
215	36	4/4/2014	WG1-20	150	150	26	1000	1000	463.875	463.425	16.88	19.59	9.94E-08	0.27	0.37	2	1200	0.15	
216	36	4/4/2014	WG1-20	150	149	26	1100	1100	462.8	459.953	20.37	22.94	6.65E-07	0.50	1.12	2	1200	0.15	
217	37	4/7/2014	WG1-21	300	303	26	800	800	464.971	464.961	5.13	7.39	2.64E-09	0.21	0.22	2	1200	0.19	
218	37	4/7/2014	WG1-21	300	304	26	850	850	464.906	464.893	7.67	10.43	2.81E-09	0.23	0.23	2	1200	0.19	
220	37	4/7/2014	WG1-21	300	289	26	950	950	464.763	464.589	13.84	16.72	3.61E-08	0.26	0.30	2	1200	0.19	
221	37	4/7/2014	WG1-21	300	284	26	1000	1000	464.502	463.907	16.91	19.73	1.26E-07	0.32	0.44	2	1200	0.19	
222	37	4/7/2014	WG1-21	300	309	26	1100	1100	463.309	458.402	20.23	22.94	1.09E-06	0.57	1.62	2	1200	0.19	
225	38	4/8/2014	WG1-22	15	8	26	950	950	456.228	456.222	13.87	16.60	1.34E-09	0.24	0.24	2	1200	0.17	
226	38	4/8/2014	WG1-22	15	8	26	1000	1000	456.161	456.086	16.97	19.81	1.61E-08	0.26	0.27	2	1200	0.17	
227	38	4/8/2014	WG1-22	15	8	25	1100	1100	455.946	455.677	20.07	22.89	5.81E-08	0.30	0.36	2	1200	0.17	
234	40	6/30/2014	WG1-24	500	475	0	850	850	463.864	463.718	3.99	6.77	3.14E-08	0.25	0.28	2	1200	0.25	
235	40	6/30/2014	WG1-24	500	614	0	900	900	463.645	463.403	7.07	9.90	5.12E-08	0.30	0.35	2	1200	0.25	
236	40	6/30/2014	WG1-24	500	520	0	950	950	463.316	462.816	10.12	12.93	1.07E-07	0.37	0.48	2	1200	0.25	
237	40	6/30/2014	WG1-24	500	520	0	1000	1000	462.648	461.181	13.25	16.01	3.19E-07	0.51	0.83	2	1200	0.25	
238	40	6/30/2014	WG1-24	500	519	0	1050	1050	460.878	456.168	16.27	19.11	1.00E-06	0.89	1.91	2	1200	0.25	
240	41	7/1/2014	WG1-25	1000	988	0	850	850	464.032	463.951	4.46	6.31	2.62E-08	0.25	0.27	2	1200	0.18	

Test Data Number	Day Number	Test Date	Specimen ID	Water Pressure		H2 Pressure	Temperature		Weight		Time in the Test		Oxidation Rate	Burn off %		Sample Preparation		Weight Loss on Outgassing	Notes
				target	actual		target	actual	before	after	before	after		before	after	duration	temperature		
				Pa	Pa	Pa	°C	°C	mg	mg	hr	hr	s <sup>-1</sup>	%	%	h	°C	mg	
241	41	7/1/2014	WG1-25	1000	712	0	900	900	464.156	463.95	7.58	10.39	4.39E-08	0.22	0.27	2	1200	0.18	
242	41	7/1/2014	WG1-25	1000	738	0	950	950	463.683	463.353	11.44	13.43	9.93E-08	0.33	0.40	2	1200	0.18	
243	41	7/1/2014	WG1-25	1000	981	0	1000	1000	463.183	461.502	13.76	16.41	3.80E-07	0.43	0.79	2	1200	0.18	
244	41	7/1/2014	WG1-25	1000	944	0	1050	1050	460.798	454.859	16.99	19.61	1.37E-06	0.95	2.22	2	1200	0.18	
247	42	7/30/2014	WG1-27	100	95	0	850	850	466.431	466.355	4.17	8.00	1.18E-08	0.25	0.20	1	1200	0.26	
248	42	7/30/2014	WG1-27	100	98	26	850	850	465.3	465.263	10.39	20.73	2.14E-09	0.49	0.50	1	1200	0.26	
249	42	7/30/2014	WG1-27	100	96	22	850	850	465.253	465.137	21.64	26.02	1.58E-08	0.50	0.56	1	1200	0.26	
250	42	7/30/2014	WG1-27	100	96	25	850	850	465.093	465.033	28.92	37.39	4.23E-09	0.54	0.55	1	1200	0.26	
251	42	7/30/2014	WG1-27	100	93	0	850	850	465.014	464.769	38.64	48.00	1.56E-08	0.56	0.61	1	1200	0.26	
252	43	8/6/2014	WG1-28	100	100	0	850	850	464.83	464.582	3.22	10.97	1.91E-08	0.26	0.31	2	1200	0.17	
253	43	8/6/2014	WG1-28	100	100	25	850	850	464.511	464.435	12.35	21.41	5.02E-09	0.33	0.35	2	1200	0.17	
254	43	8/6/2014	WG1-28	100	100	0	850	850	464.428	464.312	21.88	25.35	2.00E-08	0.35	0.37	2	1200	0.17	
255	43	8/6/2014	WG1-28	100	99	26	850	850	464.3	464.229	25.78	33.22	5.71E-09	0.37	0.39	2	1200	0.17	
256	44	8/8/2014	WG1-29	100	102	0	850	850	466.76	466.582	3.26	10.19	1.53E-08	0.22	0.26	1	1200	0.07	
257	44	8/8/2014	WG1-29	100	102	13	850	850	466.544	466.454	12.07	22.56	5.11E-09	0.27	0.29	1	1200	0.07	
258	44	8/8/2014	WG1-29	100	102	25	850	850	466.444	466.414	24.44	28.09	4.89E-09	0.29	0.30	1	1200	0.07	
259	44	8/8/2014	WG1-29	100	102	42	850	850	466.407	466.368	28.93	35.49	3.54E-09	0.30	0.31	1	1200	0.07	
260	44	8/8/2014	WG1-29	100	102	0	850	850	466.351	466.078	36.90	46.27	1.74E-08	0.31	0.37	1	1200	0.07	
261	44	8/8/2014	WG1-29	200	215	0	850	850	466.024	465.787	47.49	55.17	1.84E-08	0.38	0.43	1	1200	0.07	
262	44	8/8/2014	WG1-29	200	213	44	850	850	465.753	465.682	56.95	68.10	3.80E-09	0.44	0.45	1	1200	0.07	
263	44	8/8/2014	WG1-29	200	212	21	850	850	465.661	465.59	70.72	78.78	5.25E-09	0.46	0.47	1	1200	0.07	
264	45	8/12/2014	WG1-30	100	31	0	850	850	465.485	465.392	3.15	7.24	1.36E-08	0.26	0.28	1	1200	0.144	
265	45	8/12/2014	WG1-30	100	31	13	850	850	465.377	465.368	8.70	11.20	2.15E-09	0.28	0.28	1	1200	0.144	
266	45	8/12/2014	WG1-30	100	31	25	850	850	465.365	465.339	11.74	20.03	1.87E-09	0.28	0.29	1	1200	0.144	
267	45	8/12/2014	WG1-30	100	31	39	850	850	465.338	465.326	20.52	24.36	1.87E-09	0.29	0.29	1	1200	0.144	
268	45	8/12/2014	WG1-30	100	31	0	850	850	465.305	465.22	26.12	28.80	1.89E-08	0.30	0.31	1	1200	0.144	
269	45	8/12/2014	WG1-30	100	52	0	850	850	465.202	465.118	29.36	31.91	1.97E-08	0.32	0.34	1	1200	0.144	
270	45	8/12/2014	WG1-30	100	52	39	850	850	465.105	465.094	33.01	35.56	2.58E-09	0.34	0.34	1	1200	0.144	
271	45	8/12/2014	WG1-30	100	52	25	850	850	465.09	465.036	36.42	45.13	3.70E-09	0.34	0.35	1	1200	0.144	
272	45	8/12/2014	WG1-30	100	52	13	850	850	465.027	464.985	46.60	51.04	5.65E-09	0.36	0.36	1	1200	0.144	
275	46	8/15/2014	WG1-31	15	14	25	850	850	469.05	469.042	12.39	18.33	7.98E-10	0.23	0.24	1	1200	0.097	
277	46	8/15/2014	WG1-31	50	52	25	850	850	469.037	469.019	22.48	27.74	2.03E-09	0.24	0.24	1	1200	0.097	
278	46	8/15/2014	WG1-31	100	105	26	850	850	469.01	468.938	28.50	35.88	5.78E-09	0.24	0.26	1	1200	0.097	
279	46	8/15/2014	WG1-31	30	30	25	850	850	468.937	468.911	36.89	46.14	1.67E-09	0.26	0.26	1	1200	0.097	
280	46	8/15/2014	WG1-31	150	150	28	850	850	468.881	468.786	46.99	51.82	1.17E-08	0.27	0.29	1	1200	0.097	
281	46	8/15/2014	WG1-31	150	154	28	850	850	468.786	468.703	51.82	58.44	7.43E-09	0.29	0.31	1	1200	0.097	
282	46	8/15/2014	WG1-31	3	5	25	850	850	468.721	468.706	59.62	70.73	8.00E-10	0.30	0.31	1	1200	0.097	
283	47	8/25/2014	WG1-32	15	15	26	800	800	455.577	455.569	5.83	14.08	5.91E-10	0.26	0.26	2	1200	0.15	
284	47	8/25/2014	WG1-32	15	15	26	850	850	455.496	455.472	14.89	24.11	1.59E-09	0.27	0.28	2	1200	0.15	
285	47	8/25/2014	WG1-32	15	15	26	900	900	455.393	455.365	25.13	34.36	1.85E-09	0.30	0.30	2	1200	0.15	
286	47	8/25/2014	WG1-32	15	15	26	950	950	455.285	455.207	34.99	44.46	5.03E-09	0.32	0.34	2	1200	0.15	
287	48	9/3/2014	WG1-33	30	30	25	800	800	462.61	462.59	6.36	14.26	1.44E-09	0.239	0.243	2	1200	0.207	
288	48	9/3/2014	WG1-33	30	30	25	850	850	462.53	462.49	15.17	24.17	2.74E-09	0.256	0.265	2	1200	0.207	
289	48	9/3/2014	WG1-33	30	30	25	900	900	462.42	462.35	25.08	34.45	4.36E-09	0.279	0.294	2	1200	0.207	
290	48	9/3/2014	WG1-33	30	30	25	950	950	462.28	462.10	35.04	44.59	1.16E-08	0.309	0.349	2	1200	0.207	
291	49	12/30/2014	WG1-34	30	30	0	800	800	468.207	468.247	10.34	15.33	6.30E-09	0.020	0.01	1	1200	0.063	
292	49	12/30/2014	WG1-34	30	30	0	850	850	468.235	468.143	15.82	25.31	9.81E-09	0.014	0.03	1	1200	0.063	
293	49	12/30/2014	WG1-34	30	30	0	900	900	468.226	468.067	26.13	35.55	1.47E-08	0.016	0.05	1	1200	0.063	
294	49	12/30/2014	WG1-34	30	30	0	950	950	468.225	467.903	35.88	45.69	2.40E-08	0.016	0.08	1	1200	0.063	
295	50	1/1/2015	WG1-34	12	12	0	850	850	468.307	468.226	9.69	14.45	9.22E-09	0.00	0.02	1	1200	0.06	
296	50	1/1/2015	WG1-34	12	12	0	900	900	468.233	468.191	14.78	19.51	1.37E-08	0.01	0.02	1	1200	0.06	
297	51	1/5/2015	WG1-34	3	3	0	800	800	468.273	468.253	4.42	9.45	5.54E-09	0.01	0.02	1	1200	0.092	
298	51	1/5/2015	WG1-34	3	3	0	850	850	468.237	468.22	9.81	14.48	1.02E-08	0.01	0.02	1	1200	0.092	

Test Data Number	Day Number	Test Date	Specimen ID	Water Pressure		H2 Pressure	Temperature		Weight		Time in the Test		Oxidation Rate	Burn off %		Sample Preparation		Weight Loss on Outgasing	Notes
				target	actual		target	actual	before	after	before	after		before	after	duration	temperature		
				Pa	Pa	Pa	°C	°C	mg	mg	hr	hr	s <sup>-1</sup>	%	%	h	°C	mg	
299	51	1/5/2015	WG1-34	3	3	0	900	900	468.233	468.197	14.81	19.63	1.27E-08	0.01	0.02	1	1200	0.092	
300	51	1/5/2015	WG1-34	3	3	0	950	950	468.229	468.181	19.93	24.60	1.51E-08	0.01	0.02	1	1200	0.092	
301	52	1/7/2016	WG1-34	3	3	0	800	800	468.686	468.276	5.33	9.94	3.09E-09	0.01	0.02	1	1200	0.081	
302	52	1/7/2016	WG1-34	3	3	0	850	850	468.239	468.228	10.25	14.95	9.09E-09	0.01	0.02	1	1200	0.081	
303	52	1/7/2016	WG1-34	3	3	0	900	900	468.234	468.188	15.26	20.05	1.39E-08	0.01	0.02	1	1200	0.081	
304	52	1/7/2016	WG1-34	3	3	0	950	950	468.229	468.165	20.32	25.18	1.65E-08	0.01	0.02	1	1200	0.081	

**REJECTED DATA**

239	40	6/30/2014	WG1-24	500	530	0	1100	1100	455.242	441.4	19.41	22.27	2.95E-06	2.11	5.08	2	1200	0.25	N1
245	41	7/1/2014	WG1-25	1000	702	0	1100	1100	453.542	442.934	19.95	21.74	3.63E-06	2.51	4.79	2	1200	0.18	N1
246	41	7/1/2014	WG1-25	1000	1447	0	1100	1100	442.934	430.093	21.74	22.84	7.32E-06	4.79	7.55	2	1200	0.18	N1
163	28	3/5/2014	AG3-15	30	15	26	800	800	462.756	462.756	4.82	7.36	0.00E+00	0.18	0.18	2	1200	0.16	N2
169	29	3/6/2014	AG3-16	30	30	26	800	800	470.752	470.749	4.68	7.34	6.65E-10	0.17	0.17	2	1200	0.12	N3
170	29	3/6/2014	AG3-16	30	15	25	850	850	470.696	470.7	7.73	10.41	-8.81E-10	0.18	0.18	2	1200	0.12	N4
175	30	3/7/2014	AG3-17	50	52	26	800	800	466.475	466.491	4.60	7.36	-3.45E-09	0.19	0.18	2	1200	0.15	N4
188	32	3/25/2014	AG3-20	150	151	26	850	850	452.259	452.272	7.67	10.43	-2.89E-09	0.24	0.24	2	1200	0.22	N4
193	33	4/1/2014	WG1-17	100	102	26	800	800	467.009	466.98	5.13	7.39	7.63E-09	0.20	0.21	2	1200	0.17	N5
194	33	4/1/2014	WG1-17	100	101	25	850	850	466.953	466.985	7.70	10.46	-6.90E-09	0.22	0.21	2	1200	0.17	N4
199	34	4/2/2014	WG1-18	50	51	26	800	800	463.408	463.386	5.51	7.42	6.90E-09	0.20	0.20	2	1200	0.18	N5
200	34	4/2/2014	WG1-18	50	51	26	850	850	463.34	463.361	7.70	10.55	-4.42E-09	0.21	0.21	2	1200	0.18	N4
205	35	4/3/2014	WG1-19	30	30	26	800	800	463.123	463.123	5.53	7.38	0.00E+00	0.20	0.20	2	1200	0.17	N2
206	35	4/3/2014	WG1-19	30	30	26	850	850	463.075	463.114	7.68	10.47	-8.39E-09	0.21	0.20	2	1200	0.17	N4
207	35	4/3/2014	WG1-19	30	30	26	900	900	463.063	463.066	10.75	13.55	-6.43E-10	0.21	0.21	2	1200	0.17	N4
209	35	4/3/2014	WG1-19	30	30	26	1000	1000	465.219	462.71	16.95	19.80	5.26E-07	-0.25	0.29	2	1200	0.17	N3
211	36	4/4/2014	WG1-20	150	152	26	800	800	464.249	464.24	4.88	7.39	2.15E-09	0.19	0.19	2	1200	0.15	N3
212	36	4/4/2014	WG1-20	150	150	26	850	850	464.191	464.215	7.81	10.49	-5.36E-09	0.21	0.20	2	1200	0.15	N4
223	38	4/8/2014	WG1-22	15	22	26	850	850	456.287	456.317	7.67	10.43	-6.62E-09	0.23	0.22	2	1200	0.17	N4
224	38	4/8/2014	WG1-22	15	8	26	900	900	456.266	456.283	10.74	13.59	-3.63E-09	0.23	0.23	2	1200	0.17	N4
229	39	4/9/2014	WG1-23	30	4	96	850	850	469.615	469.638	7.69	10.45	-4.93E-09	0.11	0.10	2	1200	0.26	N4
230	39	4/9/2014	WG1-23	30	4	96	900	900	469.638	469.655	10.79	13.46	-3.77E-09	0.10	0.10	2	1200	0.26	N4
231	39	4/9/2014	WG1-23	30	4	96	950	950	469.634	469.655	13.89	16.62	-4.55E-09	0.10	0.10	2	1200	0.26	N4
273	46	8/15/2014	WG1-31	3	4	85	850	850	469.07	469.062	3.49	9.17	5.21E-10	0.23	0.23	1	1200	0.097	N3
274	46	8/15/2014	WG1-31	3	4	85	850	850	469.062	469.064	9.17	11.04	-6.33E-10	0.23	0.23	1	1200	0.097	N4
187	32	3/25/2014	AG3-20	150	152	26	800	800	452.311	452.31	5.38	7.39	3.06E-10	0.23	0.23	2	1200	0.22	N3
219	37	4/7/2014	WG1-21	300	296	26	900	900	464.84	464.828	10.74	13.56	2.54E-09	0.24	0.25	2	1200	0.19	N1
276	46	8/15/2014	WG1-31	15	8	25	850	850	469.042	469.041	18.33	21.72	1.75E-10	0.24	0.24	1	1200	0.097	N3
171	29	3/6/2014	AG3-16	30	29	26	900	900	470.671	470.67	12.67	13.59	6.41E-10	0.19	0.19	2	1200	0.12	N6
228	39	4/9/2014	WG1-23	30	4	96	800	800	469.592	469.613	4.56	7.26	-4.60E-09	0.11	0.11	2	1200	0.26	N3
232	39	4/9/2014	WG1-23	30	4	96	1000	1000	469.65	469.601	16.96	19.63	1.09E-08	0.10	0.11	2	1200	0.26	N3
233	39	4/9/2014	WG1-23	30	4	96	1100	1100	469.581	469.517	20.15	22.85	1.40E-08	0.12	0.13	2	1200	0.26	N3
181	31	3/14/2014	AG3-19	100	101	26	800	800	459.769	459.772	5.30	7.25	-9.29E-10	0.19	0.19	2	1200	0.22	N4
43	8	1/9/2014	WG1-12	15	15	0	800	800	463.377	463.249	4.13	6.72	2.96E-08	0.18	0.21	2	1200	0.14	N5

N1 = unstable weight readings; N2 = apparent “zero” rate; N3 = experimental errors; N4 = apparent “negative” rate; N5 = uncommon trend; N6 = unsteady state

**Table A-3:** Fitted parameter estimates and standard errors provided by SAS

SAS Parameters	Estimate	Standard Error	Confidence intervals		Gradient	L-H Parameters	Estimate	Confidence intervals	
			Lower	Upper				Lower	Upper
All Temperatures (800 - 1100 °C)									
a1	-12.468	1.3374	-15.1542	-9.7819	3.45E-06	A1	3.85E-06	2.62E-07	5.65E-05
b1	-7.3964	1.7409	-10.8932	-3.8996	4.76E-06	A2	4.00E-08	1.06E-09	1.51E-06
a2	-17.0341	1.8085	-20.6667	-13.4016	-5.90E-06	A3	5.79E-07	2.74E-08	1.22E-05
b2	22.4502	2.2377	17.9558	26.9447	-5.18E-06	E1	61,494	90,566	32,421
a3	-14.3624	1.5182	-17.4118	-11.313	-3.62E-06	E2	-186,651	-149,285	-224,018
b3	14.7806	1.9233	10.9175	18.6436	-4.77E-06	E3	-122,886	-90,768	-155,003
s2u	0.1952	0.04352	0.1078	0.2826	0.00001				
s2	0.4514	0.02187	0.4074	0.4953	-0.00004				
Low Temperatures (800 - 950 °C)									
a1	-25.6475	9.2171	-44.1605	-7.1345	8.66E-06	A1	7.27E-12	6.63E-20	7.97E-04
b1	8.9619	11.2904	-13.7156	31.6394	7.76E-06	A2	1.08E-10	7.11E-19	1.64E-02
a2	-22.9484	9.3798	-41.7883	-4.1085	-0.00002	A3	4.73E-10	3.65E-18	6.13E-02
b2	30.5303	11.4679	7.4963	53.5643	-0.00002	E1	-74,509	114,031	-263,050
a3	-21.4714	9.2997	-40.1505	-2.7923	4.70E-06	E2	-253,829	-62,324	-445,334
b3	24.3938	11.3949	1.5065	47.281	4.91E-06	E3	-202,810	-12,525	-393,094
s2u	0.2623	0.04052	0.1809	0.3437	0.000027				
s2	0.3265	0.01981	0.2867	0.3663	0.00022				
High Temperatures (900 - 1100 °C)									
a1	-12.6576	1.3106	-15.2972	-10.018	-0.00009	A1	3.18E-06	2.27E-07	4.46E-05
b1	-7.445	1.766	-11.0019	-3.8882	-0.00006	A2	8.95E-13	6.24E-15	1.28E-10
a2	-27.7424	2.4654	-32.7079	-22.7768	-0.0002	A3	3.99E-10	1.55E-11	1.03E-08
b2	35.6533	3.055	29.5002	41.8064	-0.00016	E1	61,898	91,470	32,326
a3	-21.6432	1.6127	-24.8913	-18.3951	0.000223	E2	-296,422	-245,265	-347,578
b3	23.6152	2.1001	19.3854	27.845	0.000167	E3	-196,337	-161,170	-231,503
s2u	0.2305	0.03632	0.1574	0.3037	0.000439				
s2	0.2874	0.01868	0.2498	0.325	-0.00137				

Units: A<sub>1</sub> (Pa<sup>-1</sup>s<sup>-1</sup>); A<sub>2</sub> (Pa<sup>-0.5</sup>); A<sub>3</sub> (Pa<sup>-1</sup>); E<sub>1</sub>, E<sub>2</sub>, E<sub>3</sub> (J/mol)



**DISTRIBUTION LIST****Oak Ridge National Laboratory**

Timothy Burchell	<a href="mailto:burchelltd@ornl.gov">burchelltd@ornl.gov</a>
Peter Tortorelli	<a href="mailto:tortorellipf@ornl.gov">tortorellipf@ornl.gov</a>
Yutai Katoh	<a href="mailto:katohy@ornl.gov">katohy@ornl.gov</a>
Cristian Contescu	<a href="mailto:contescuci@ornl.gov">contescuci@ornl.gov</a>
Weiju Ren	<a href="mailto:renw@ornl.gov">renw@ornl.gov</a>
John Hunn	<a href="mailto:hunnjd@ornl.gov">hunnjd@ornl.gov</a>
Nidia Gallego	<a href="mailto:gallegonc@ornl.gov">gallegonc@ornl.gov</a>
Sam Sham	<a href="mailto:shamt@ornl.gov">shamt@ornl.gov</a>

**Idaho National Laboratory**

David Petti	<a href="mailto:David.Petti@inl.gov">David.Petti@inl.gov</a>
William Windes	<a href="mailto:William.Windes@inl.gov">William.Windes@inl.gov</a>
Laurence Hull	<a href="mailto:Laurence.Hull@inl.gov">Laurence.Hull@inl.gov</a>
Rebecca Smith	<a href="mailto:Rebecca.Smith@inl.gov">Rebecca.Smith@inl.gov</a>
Robert Bratton	<a href="mailto:Robert.Bratton@inl.gov">Robert.Bratton@inl.gov</a>
David Jensen	<a href="mailto:David.Jensen@inl.gov">David.Jensen@inl.gov</a>
Joshua Kane	<a href="mailto:Joshua.Kane@inl.gov">Joshua.Kane@inl.gov</a>

**Department of Energy**

William Corwin	<a href="mailto:William.Corwin@Nuclear.Energy.gov">William.Corwin@Nuclear.Energy.gov</a>
Thomas O'Connor	<a href="mailto:Tom.OConnor@Nuclear.Energy.gov">Tom.OConnor@Nuclear.Energy.gov</a>
Carl Sink	<a href="mailto:Carl.Sink@Nuclear.Energy.gov">Carl.Sink@Nuclear.Energy.gov</a>